Available online at www.sciencedirect.com

SCIENCE @ DIRECT®

ELSEVIER

Coordination Chemistry Reviews 246 (2003) 53–71

COORDINATION CHEMISTRY REVIEWS

www.elsevier.com/locate/ccr

Design of hydrogen bonded networks based on organometallic sandwich compounds

Dario Braga [a,*], Lucia Maini [a], Marco Polito [a],
Emilio Tagliavini [a], Fabrizia Grepioni [b,*]

[a] *Dipartimento di Chimica G. Ciamician, Università degli Studi di Bologna, Via F. Selmi 2, 40126 Bologna, Italy*
[b] *Dipartimento di Chimica, Università degli Studi di Sassari, Via Vienna 2, 07100 Sassari, Italy*

Contents

Abstract . . . 53
1. Introduction . . . 54
2. Organometallic crystal engineering with ionic building blocks . . . 55
    2.1. Strategies to obtain hydrogen bonded networks involving ions . . . 55
3. Hydrogen bonded networks templated by organometallic sandwich units . . . 56
    3.1. Columnar aggregation . . . 56
    3.2. Intercalation . . . 57
    3.3. Brickwall aggregation . . . 58
    3.4. Honeycomb aggregation . . . 59
    3.5. Interpenetration and folding . . . 60
    3.6. Hinged folding and embracing . . . 60
    3.7. Partial conclusions . . . 61
4. Hydrogen bonded networks formed by organometallic sandwich units . . . 62
    4.1. Hybrid organic–organometallic crystals . . . 62
    4.2. Mixed-metal hydrogen bonded networks . . . 64
    4.3. Neutral and cationic acids of $[(\eta^6\text{-}C_6H_5COOH)_2Cr]$ . . . 67
    4.4. Zwittwerionic and cationic acids of $[(\eta^5\text{-}C_5H_4COOH)_2Co]^+$ . . . 68
5. Conclusions and outlook . . . 70
Acknowledgements . . . 70
References . . . 70

Abstract

The design, construction and evaluation of hybrid organic–organometallic and inorganic–organometallic crystalline materials held together by *charge assisted* hydrogen bonding interactions are described. It is shown that the convolution of the properties typical of coordination complexes (topology, oxidation and charge states etc.) with the extramolecular bonding capacity of ligands carrying hydrogen bonding groups allows one to prepare molecular and materials with desired architectures. The ionic or neutral nature of the building blocks can be utilized not only to control the strength of intermolecular bonding, but also to attain structure–function relationships and desired properties. In the case of organometallic species it is possible to vary in a controlled way both the redox properties of the metal centers and/or the acid/base behavior of the ligands. The possibility of utilizing the same building blocks in different neutral and ionic conditions can be exploited to construct complex structures for a variety of supramolecular applications.

Keywords: Organometallic crystal engineering; Hydrogen bond; Solid-state reactivity

---

[*] Corresponding authors. Tel.: +39-51-209-9555; fax: +39-51-209-9456 (D.B.).
E-mail address: dbraga@ciam.unibo.it (D. Braga).

0010-8545/$ – see front matter © 2003 Elsevier B.V. All rights reserved.
doi:10.1016/S0010-8545(03)00108-5

1. Introduction

The engineering of molecular crystals [1] is at the hinge between supramolecular chemistry [2] and materials chemistry [3]. Both disciplines are concerned with the utilization of non-covalent interactions to pre-determine chemical and physical properties of the supramolecular aggregates [4]. In fact, there is not much conceptual difference between a supermolecule, whose *collective* functions and properties differ from—but depend on—those of the individual components, and a crystalline material, whose collective properties result from the aggregation of a very large number of identical subunits [5]. Thus the design and construction of a molecular solid can be seen as the construction of a solid supermolecule, whose collective functions depend on the aggregation via *intermolecular* bonds of two or more component units.

At variance with conventional synthetic procedures, however, the construction of materials with predefined physical properties or destined to predefined applications and uses require *crystal-oriented synthetic strategies* [6]. In this respect a distinction needs to be made between crystalline solids in which the principal interactions holding crystals together are covalent, van der Waals and/or ionic, and solids where ligand–metal coordination networks are present. While covalent or coordination solids exploit two-electron σ-bonds, molecular materials owe their stability to the network of generally weaker non-covalent interactions between molecular building blocks. Since the cohesion of covalent and coordination solids depends on interactions that require much more energy to be broken and formed than those present in molecular solids, the synthetic strategies that can be adopted to make covalent (and coordination) crystalline materials are different from those required when molecules or molecular ions are involved [7].

In the following, the epithet ‘molecular’ will be used in a broad sense, encompassing both neutral and ionic systems based on the working assumption that are ‘molecular’ all those aggregates of atoms that retain their own chemical identity in gas-phase or solution. On this premise we will call *intermolecular* all those types of secondary inter-ionic or inter-molecular *non-covalent* interactions (e.g. electrostatic, hydrogen bonds, and van der Waals interactions) that do not imply two-electrons σ-bonds. More specifically, this article deals with the construction of hydrogen bonded networks involving coordination complexes, mainly of organometallic nature, where the hydrogen bonding interactions are between ‘classical’ donor and acceptor groups, e.g. –COOH, –OH, –CONHR, etc. [8], while less attention will be given to weak hydrogen bonding interactions [9]. These latter interactions, albeit important in the *fine tuning* of the supramolecular architectures are, generally speaking, more difficult to control than ‘strong’ interactions with clearly defined, reproducible and transferable directionality properties. Hydrogen bonding has been the subject of many review articles and books and will not be dealt with in detail on this occasion. The reader is addressed to Ref. [10] for some additional entry points.

Less attention, however, has been paid to the *convolution* of hydrogen bonding interactions with the Coulombic field in ionic crystals. The role of Coulombic forces arising from the presence of ions in the crystal structure is, obviously, extremely relevant in determining crystal cohesion. Even though Coulombic interactions often account for most of the cohesive energy in ionic crystals, the exploitation of these interactions to design and construct crystals is complicated by the tendency for an ion to surround itself with ions of opposite sign (e.g. NaCl). This is not always a desired effect, as many interesting properties arise from anisotropic distributions of building blocks. A higher degree of control can instead be attained when hydrogen bonding interactions are convoluted with Coulombic interactions [11]. This article will focus mainly on the diverse architectures that can be obtained by means of hydrogen bonding interactions between ionic species.

It is a fact that hydrogen bonds between ions are widely employed to obtain predefined crystalline architectures [12]. There are several reasons for this choice:

i) inter-ionic hydrogen bonds are easily obtained in crystal synthesis via proton transfer associated with acid–base reactions (see below);
ii) they *combine* hydrogen bond directionality with the strength of Coulombic forces (which are stronger than ion–dipole or dipole–dipole forces but less directional and less useful as design tools);
iii) the use of ions permits a much greater choice of components, which, in the case of transition metal complexes, may not only possess different topologies, but also different bonding and electronic characteristics.
iv) the simultaneous use of hydrogen bonding interactions and of Coulombic interactions (i.e. hydrogen bonds *immersed* in an electrostatic field) affords crystal properties that are a *convolution* of those of hydrogen bonded molecular systems and of those of ionic salts.

The relationship between the energetic contribution of the hydrogen bonding interactions and the Coulombic terms has led to controversial interpretations (at least in the case of hydrogen bonds between ions of the same charge) [13]. The discussion of this aspect of the problem, albeit interesting, is outside the scope of this review and will only briefly be dealt with in the following section.

Since we are interested in *using* hydrogen bonds to *make* solids, it remains to be pointed out that, while hydrogen bonding crystal engineering with organic molecules is mainly focused on the preparation of molecular crystals formed of neutral building blocks, charged systems are much more frequent when coordination complexes or organometallic compounds are employed, because of the often ionic nature of the building blocks [14].

2. Organometallic crystal engineering with ionic building blocks

Since the hydrogen bond has a fundamentally electrostatic nature [15], the presence of ionic charges on the building blocks can be exploited to strengthen the interaction [16]. *Charge assistance* to hydrogen bond is the enhancement of donor and acceptor polarity (whether involving atoms or groups of atoms) by a combined use of cationic donors and anionic acceptors instead of neutral systems, i.e. $\mathrm{X{-}H}^{(+)}\cdots\mathrm{Y}^{(-)}$ versus $\mathrm{X{-}H}\cdots\mathrm{Y}$ [17]. The favorable location of ionic charges enhances proton acidity *and* acceptor basicity. It should be kept in mind, however, that ‘acidity’ or ‘basicity’ are *relative* concepts and cannot be transferred *tout-court* to the solid state; other factors may change the polarity of the X–H bond and/or the nucleophilicity of the Y acceptor [18]. If the hydrogen bond joins ions of opposite charge, more generally $^{(+)}\mathrm{X{-}H}\cdots\mathrm{Y}^{(-)}$, the bonding contribution adds to the favorable $(+)\cdots(-)$ Coulombic interaction between donor and acceptor systems, while if the ions carry the same charge, e.g. $^{(-)}\mathrm{X{-}H}\cdots\mathrm{Y}^{(-)}$, (but also $^{(+)}\mathrm{X{-}H}\cdots\mathrm{Y}^{(+)}$) the contribution reduces the repulsive electrostatic terms (e.g. $(-)\cdots(-)$ or $(+)\cdots(+)$) arising from the Coulombic interactions between like charges.

When the hydrogen bonding functional group belongs to a ligand and does not take part in coordination to the metal centers, the extramolecular bonding capacity of the molecules remains essentially unaltered with respect to that of organic molecules. This is of course not true if the hydrogen bonding donor/acceptor system interacts with the metal center. In this latter case the hydrogen bonding capacity is affected. A third relevant difference between organic and inorganic hydrogen bonding is the role of ionic charges, which becomes very relevant in systems where the ionic status can be modified via redox processes and/or via acid base reactions. In the following discussion examples of both types will be provided.

For the sake of clarity, the following discussion has been organized by grouping compounds in two main categories, namely (i) hydrogen bonded networks *templated* by organometallic units and (ii) hydrogen bonded networks *formed* by organometallic units. The two terms are self-explanatory: the former class of compounds will contain crystals where the backbone component is formed essentially of organic or inorganic building blocks interacting via hydrogen bonding, while the latter will see the direct involvement of metal complexes in the hydrogen bonding networks.

Our goals have been the following: (i) to gain insight in the factors crucial for architecture design; (ii) to prepare chiral frameworks with potential applications in non-linear optics [19]; (iii) to prepare honeycomb structures with potential applications in guest exchange, trapping, and sensing of molecules [20]; (iv) to prepare columns, layers, and pairs of paramagnetic ions with potentials in magnetic applications [21].

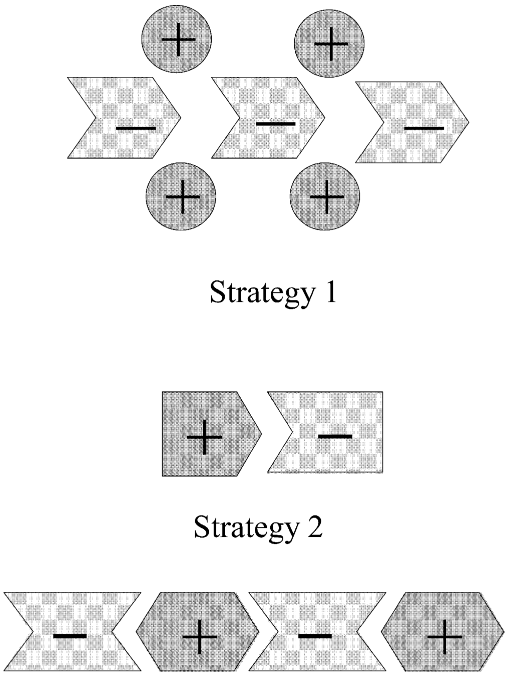

Scheme 1. Strategy 1: the base *cannot form* hydrogen bonding interactions with the acid moiety; the stability of the resulting *homo-ionic* aggregate (negative arrows) is ensured via an adequate choice of counterions (positive spheres). Strategy 2: the base *forms charge-assisted* hydrogen bonding interactions with the acidic moiety, yielding anion–cation pairs or chains in the solid state.

2.1. Strategies to obtain hydrogen bonded networks involving ions

The simplest way to obtain hydrogen bonded ionic networks is that of using—or *generating* in situ—ions that can be linked together via hydrogen bonding interactions.

There are two distinct strategies that utilize acid–base reactions to construct crystals based on charge assisted hydrogen bonds between ions (see Scheme 1):

Strategy 1: use of a base that *cannot form* hydrogen bonding interactions with the acid moiety. This is the case of the reaction between polycarboxylic acids with inorganic or organometallic hydroxides that do not carry strong acceptor/donor hydrogen bond groups. In fact, partial deprotonation of the –COOH groups leads to self-assembly of acid anions via $\mathrm{O{-}H}\cdots\mathrm{O}^{(-)}$ and $^{(-)}\mathrm{O{-}H}\cdots\mathrm{O}^{(-)}$ interactions. By choosing the number of carboxylic groups (hence the number of potential donor/acceptor systems) and the stoichiometric ratios in the acid–base reactions, one can control the formation of $\mathrm{O{-}H}\cdots\mathrm{O}^{(-)}$ and/or $^{(-)}\mathrm{O{-}H}\cdots\mathrm{O}^{(-)}$ interactions. In this latter circumstance one can speak of *homo-ionic* self-assembly. The stability of the resulting *homo-ionic* network aggregate requires an adequate choice of counterions.

Strategy 2: use of a base that *forms charge-assisted* hydrogen bonding interactions with the acidic moiety. This is the case, for instance, of nitrogen containing bases (amines, pyridines, pyrimidines, aminidines etc.) which are protonated upon reaction with polycarboxylic acid molecules, e.g. $RCOOH + NR_3 \rightarrow RCOO^{(-)} \cdots {}^{(+)}HNR_3$, leading to formation of strong $N–H^{(+)} \cdots O^{(-)}$ interactions, hence to formation of anion–cation pairs in the solid state.

However, the distinction between the two strategies is only instrumental to the discussion, since intermediate situations whereby *homo-ionic* and *hetero-ionic* hydrogen bonding interactions may coexist, e.g. $N–H^{(+)} \cdots O^{(-)}$ and ${}^{(-)}O–H \cdots O^{(-)}$, can be obtained by using a large acid:base ratio.

3. Hydrogen bonded networks templated by organometallic sandwich units

This section is devoted to the description of hydrogen bonded networks obtained via *strategy 1*.

We will follow a path of increasing building block complexity; it will be shown that the size and shape, and *extramolecular bonding capacity*, of the organic building block can be used to control the crystal architecture. Although no hard and fast rule can be applied, the aggregation of partially deprotonated polycarboxylic acids or poly-alcohols follows a sort of *aufbau* hierarchy: (i) priority goes to the maximization of the number of hydrogen bonding interactions between strong donors and acceptors, (ii) a compromise is also required between space-filling and charge equalization, (iii) after all strong interactions have been accommodated, weaker $C–H \cdots O$ and similar interactions are also optimized. These criteria are essentially those put forward by Etter [18]. Even though the stability of the aggregate depends also on the topological features of the counterions, ${}^{(-)}O–H \cdots O^{(-)}$ hydrogen bonding interactions between building blocks of like charges (as it is generally the case of the compounds described in this section) contribute to crystal stability by decreasing the anion–anion (or cation–cation) repulsions [22]. All crystalline materials described below are in fact constituted of *homo-ionic* networks stabilized by organometallic sandwich counterions, which, for most, can interact with the surroundings via charge assisted $C–H \cdots O$ bonds.

Table 1 shows the relationship between nature of the building block and topology of the anionic frameworks. Relevant cases will be illustrated with reference to the graphs in Scheme 2.

Table 1
Relationship between nature of the building block and topology of the anionic framework

Building block features	Type of organic acid	Superstructure features
Small and elongated	Oxalic acid	Columns
Medium and flat	Squaric acid	Intercalates
Large and flat	Phthalic acids	Brickwalls
Long and flexible	Tartaric acids	Honeycombs
Polycarboxylic acid	Trimesic, tetracarboxylic acids	Interpenetration and folding
Hinged	Binaphthols	Folding and embracing

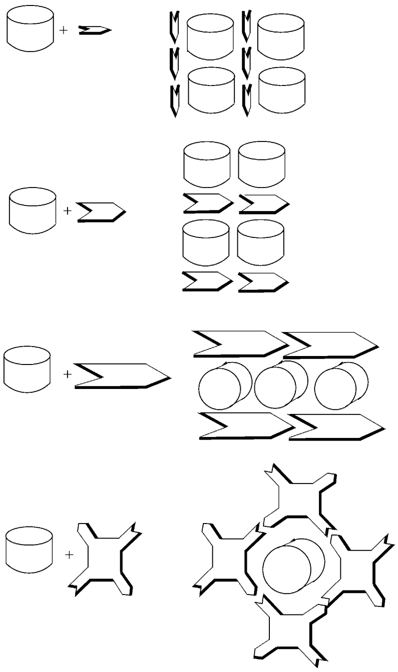

Scheme 2. The size/shape–topology relationship of organic (arrows) and organometallic (cylinders) building blocks.

The approach developed in Bologna is based on combination of redox and acid–base processes utilizing organometallic bases and polyprotic acids. For instance, the spontaneous oxidation by oxygen of the neutral complexes $[(\eta^5\text{-}C_5H_5)_2Co]$ and $[(\eta^6\text{-}C_6H_6)_2Cr]$ to $[(\eta^5\text{-}C_5H_5)_2Co]^+$ and $[(\eta^6\text{-}C_6H_6)_2Cr]^+$, respectively, generates the strongly basic anion O_2^-, which is able to fully or partially deprotonate the polyprotic acid, depending on the stoichiometric ratio [23]. Other cations that have also been used are the decamethyl derivatives $[(\eta^5\text{-}C_5Me_5)_2Fe]^+$ and $[(\eta^5\text{-}C_5Me_5)_2Co]^+$. Since the oxidation products, namely the cations $[(\eta^5\text{-}C_5H_5)_2Co]^+$ and $[(\eta^6\text{-}C_6H_6)_2Cr]^+$, are not suitable for coordination by the $–COO^{(-)}$ groups, self-assembly of the polycarboxylic acid is forced with formation of 1D, 2D or 3D *homo-ionic* framework structures around the organometallic cations. As mentioned above, the interaction between organic framework and organometallic cations is based on a profusion of charge assisted $C–H \cdots O$ bonds. Table 2 lists the compounds that have been obtained by means of this reaction strategy, together with the relevant literature entries.

3.1. Columnar aggregation

The use of the small hydrogen oxalate anion allows the construction of crystalline materials with predefined architectures involving radical cations. When oxalic acid was used with $[(\eta^5\text{-}C_5Me_5)_2Fe]^+$ and $[(\eta^6\text{-}C_6H_6)_2Cr]^+$ two crystalline compounds were obtained, namely $[(\eta^5\text{-}C_5Me_5)_2Fe]$

Table 2
Hybrid organic–organometallic superstructures obtained with *strategy 1* and relevant literature entries

Acid	Organometallic building block	Formula of the resulting system	n
Oxalic [24]	$[(\eta^5\text{-}C_5Me_5)_2Fe]$	$[(\eta^5\text{-}C_5Me_5)_2Fe][HC_2O_4]\cdot[H_2C_2O_4]_{0.5}$	**I**
Oxalic [24]	$[(\eta^6\text{-}C_6H_6)_2Cr]$	$[(\eta^6\text{-}C_6H_6)_2Cr][HC_2O_4]\cdot[H_2O]$	**II**
Squaric [25]	$[(\eta^6\text{-}C_6H_6)_2Cr]$	$[(\eta^6\text{-}C_6H_6)_2Cr][HC_4O_4]$	**III**
Squaric [25]	$[(\eta^6\text{-}C_6H_6)_2Cr]$	$\{[(\eta^6\text{-}C_6H_6)_2Cr]\}_2[C_4O_4]\cdot 6H_2O$	**IV**
Phthalic [26]	$[(\eta^5\text{-}C_5H_5)_2Co]$	$\{[(\eta^5\text{-}C_5H_5)_2Co]^+\}_4\{[C_6H_4(COOH)(COO)]^-\}_2\ [C_6H_4(COO)_2]^{2-}\cdot 4H_2O$ (**1**)	**V**
Phthalic [26]	$[(\eta^6\text{-}C_6H_6)_2Cr]$	$[(\eta^6\text{-}C_6H_6)_2Cr]^+\{[C_6H_4(COOH)(COO)]^-\ [C_6H_4(COOH)_2]\}$	**VI**
Terephthalic [26]	$[(\eta^5\text{-}C_5H_5)_2Co]$	$\{[(\eta^5\text{-}C_5H_5)_2Co]^+\}_2[C_6H_4(COO)_2]^{2-}\cdot 6H_2O$	**VII**
D,L-Tartaric [23]	$[(\eta^5\text{-}C_5H_5)_2Co]$	$[(\eta^5\text{-}C_5H_5)_2Co]^+$(D,L-$HO_2CCH(OH)CH(OH)CO_2$) (D,L-$HO_2CCH(OH)CH(OH)CO_2H)]^-$	**VIII**
L-Tartaric [23]	$[(\eta^5\text{-}C_5H_5)_2Co]$	$[(\eta^5\text{-}C_5H_5)_2Co]^+$ [(L-$HO_2CCH(OH)CH(OH)CO_2)]^-$	**IX**
Trimesic [27]	$[(\eta^5\text{-}C_5H_5)_2Co]$	$[(\eta^5\text{-}C_5H_5)_2Co]^+\ \{[(C_6H_3(COOH)_3]\ [C_6H_3(COOH)_2(COO)]\}^-\cdot 2H_2O$	**X**
R-Binaphthol [28]	$[(\eta^5\text{-}C_5H_5)_2Co]$	$[(\eta^5\text{-}C_5H_5)_2Co]\ [(R)\text{-}(+)\text{-}(HOC_{10}H_6C_{10}H_6O)]\cdot[(R)\text{-}(+)\text{-}(HOC_{10}H_6C_{10}H_6OH)]$ (**1**)	**XI**
R-Binaphthol [28]	$[(\eta^5\text{-}C_5H_5)_2Co]$	$[(\eta^5\text{-}C_5H_5)_2Co]\ [(R)\text{-}(+)\text{-}(HOC_{10}H_6C_{10}H_6O)]\cdot[(R)\text{-}(+)\text{-}(HOC_{10}H_6C_{10}H_6OH)]_{0.5}$	**XII**

$[HC_2O_4]\cdot[H_2C_2O_4]_{0.5}$, **I** and $[(\eta^6\text{-}C_6H_6)_2Cr][HC_2O_4]\cdot[H_2O]$, **II** [24]. The goal was that of obtaining a columnar aggregation of radical cations, which may lead to different magnetic couplings than obtained when the radical cations are intercalated (see below) [29]. In fact, the small dimensions of the oxalic acid unit do not allow intercalation of the anions between the C_5Me_5 rings, as otherwise observed in the cases of tetracyanoethylene (TCNE) and tetracyanoquinone (TCNQ) building blocks and also for other anions, such as chloranilic acid [29]. Formation of hydrogen oxalate chains allows maximization of the number of $O\text{–}H\cdots O$ interactions, and assists formation in the crystal edifice of cationic $C^{(+)}\text{–}C^{(+)}\text{–}C^{(+)}\text{–}C^{(+)}$ columns ($C = \text{cation}$) rather than an $A^{(-)}\text{–}C^{(+)}\text{–}A^{(-)}\text{–}C^{(+)}$ sequence ($A = \text{anion}$) associated to intercalation. Even if the $C^{(+)}\text{–}C^{(+)}\text{–}C^{(+)}\text{–}C^{(+)}$ organization leads to sizeable magnetic interactions, these are much weaker, in all examples so far tested, than those observed in the charge transfer salts obtained with TCNE and TCNQ, and no bulk magnetic behavior is observed above 2 K.

As anticipated, in crystalline compound **I** the hydrogen oxalate anions and the neutral oxalic acid molecules form linear chains (see Fig. 1a). The chains run parallel to the columns formed by the $[(\eta^5\text{-}C_5Me_5)_2Fe]^+$ and $[(\eta^5\text{-}C_5Me_5)_2Co]^+$ cations, and contain *deca*-atomic dimers formed by two hydrogen oxalate anions joined together via ${}^{(-)}O\text{–}H\cdots O^{(-)}$ interactions. The anions are not arranged in the 'usual' head-to-tail chain of the carboxylic ring, they but rather adopt a side-to-side arrangement. The hydrogen oxalate dimers are bridged together by one molecule of oxalic acid. The hydrogen oxalate/oxalic acid chain can thus be described as a $(H_2C_2O_4)\text{–}[(HC_2O_4)(HC_2O_4)]^{2-}\text{–}(H_2C_2O_4)\text{–}[(HC_2O_4)(HC_2O_4)]^{2-}$ sequence of ions bridged by neutral molecules. These chains form the backbone of the crystal structure and allow the cations to pile up as shown in Fig. 1a.

A twisted conformation is adopted by the hydrogen oxalate anion in the *bis*-benzene chromium salt $[Cr(\eta^6\text{-}C_6H_6)_2][HC_2O_4]\ [H_2O]$, **II**. A view of compound **II** along the cationic stack is shown in Fig. 1b, with the benzene ligands in close contact. The twisted hydrogen oxalate anions do not interact with each other but are linked in the chains by means of water bridges, which form complex 14-membered rings based on four hydrogen bonding interactions.

With respect to larger anions derived from polycarboxylic acids (see below), the packing of the hydrogen oxalate anions has to compromise between two (not necessarily) converging factors: the size of the anion, which is small with respect to that of the sandwich cations, and the need to preserve inter-anion hydrogen bridges in the absence of competing hydrogen bonding units on the cations.

3.2. Intercalation

A second example of deliberate *engineering* of supramolecular arrangements is provided by crystalline $[(\eta^6\text{-}C_6H_6)_2Cr]^+[HC_4O_4]^-$ **III**, obtained by reaction of squaric acid (3,4-dihydroxy-3-cyclobutene-1,2-dione, $H_2C_4O_4$) with $[(\eta^6\text{-}C_6H_6)_2Cr]$ in THF. Because of its flat shape and small dimensions the squarate anion $[HC_4O_4]^-$ was expected to be able to intercalate between the flat benzene ligands of the paramagnetic cation $[(\eta^6\text{-}C_6H_6)_2Cr]^+$. Such intercalation leads to the formation of 1D $C^{(+)}\text{–}A^{(-)}\text{–}C^{(+)}\text{–}A^{(-)}$ aggregates, comprised of alternating cation donors (C) and anion acceptors (A). As designed, the anion self-assembles into chains linked by ${}^{(-)}O\text{–}H\cdots O^{(-)}$ interactions and intercalates between the benzene ligands (π–π distance 3.375 Å see Fig. 2a). When the reaction is carried out in water, the hydrated crystalline material.

$\{[(\eta^6\text{-}C_6H_6)_2Cr]\}_2[C_4O_4]\cdot 6H_2O$ **IV** is obtained instead **IV** contains layers of organometallic cations intercalated with layers of water molecules, hydrogen bonded to squarate dianions (see Fig. 2b). All crystals contain charge-assisted $C\text{–}H^{\delta+}\cdots O^{\delta-}$ hydrogen bonds between the organometallic and the organic components, while inter-anion $O\text{–}H^{(-)}\cdots O^{(-)}$ interactions and $O\text{–}H\cdots O^{(2-)}$ interactions are present.

$[(\eta^5\text{-}C_5H_5)_2Co][HC_4O_4]$ is almost isostructural with **III**, its structure being based on π–π stacks between

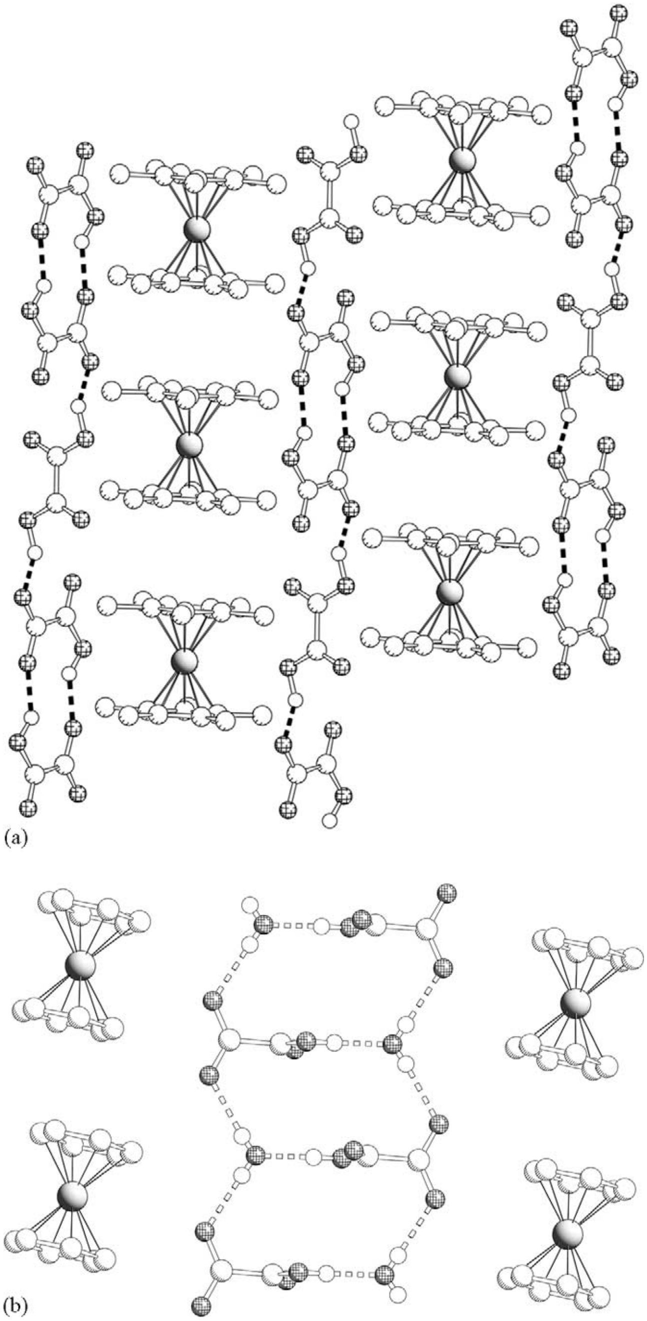

Fig. 1. (a) The ion arrangement in crystalline $[(\eta^5\text{-}C_5Me_5)_2Fe][HC_2O_4]\cdot[H_2C_2O_4]_{0.5}$, **I**. Note how the cations pile up, at inter-planar separations of 3.67 and 3.84 Å. (b) A view of compound $[(\eta^6\text{-}C_6H_6)_2Cr][HC_2O_4]\cdot[H_2O]$, **II**, showing the twisted conformation adopted by the hydrogen oxalate. H_{cation} atoms omitted for clarity.

the benzene ligands and the hydrogen squarate anionic chains.

Contrary to most organic salts of $[(\eta^6\text{-}C_6H_6)_2Cr]^+$ and $[(\eta^5\text{-}C_5H_5)_2Co]^+$ which are yellow, crystals **III** are orange in color. Reflectance spectra measured on the crystalline material **III** show the presence of an intense tail, which was assigned to a charge transfer transition via the $[(\eta^6\text{-}C_6H_6)_2Cr]^+/[HC_4O_4]^-$ π-stacking interactions [25].

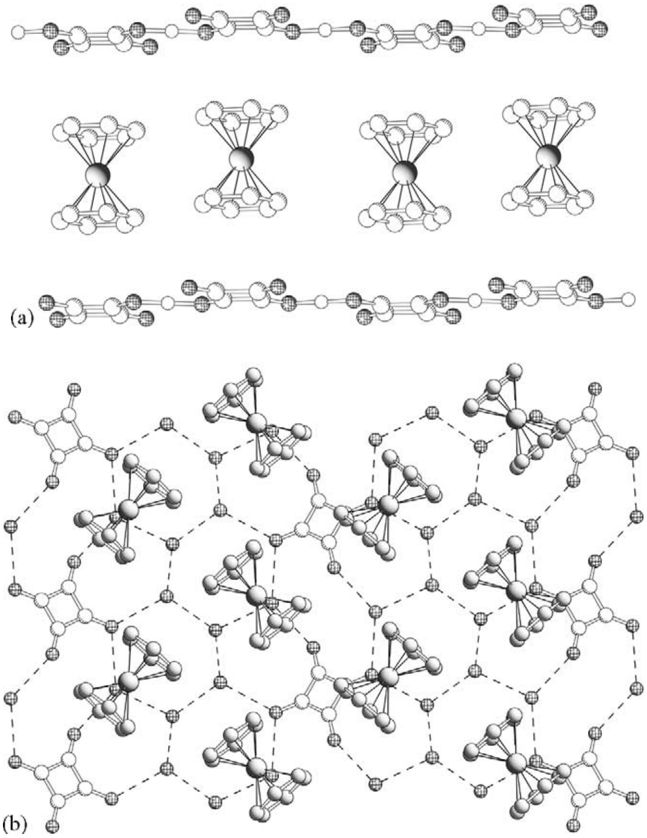

Fig. 2. Packing arrangement in crystalline **III**: representation of a row of cations encapsulated between two $\{[HSQA]^-\}_n$ ribbons (a). The corrugated layer formed by the dianions $C_4O_4^{2-}$ and water molecules and the cations on top in **IV**(b). H_{cation} atoms omitted for clarity.

3.3. *Brickwall aggregation*

When the size of hydrogen bonding organic units exceeds that of the carbocyclic ligands forming the cations, intercalation becomes again impossible, although for a different reason than in the case of the hydrogen oxalate building block. This is demonstrated by the use of flat and large diacids, such as phthalic acid, $[C_6H_4\text{-}1,2\text{-}(COOH)_2]$, and terephthalic acid, $[C_6H_4\text{-}1,4\text{-}(COOH)_2]$. These two acids when reacted with water solutions of the hydroxides $[(\eta^5\text{-}C_5H_5)_2Co]^+[OH]^-$ and $[(\eta^6\text{-}C_6H_6)_2Cr]^+[OH]^-$, produced in situ by oxidation of the parent neutral molecules as discussed before.

Though chemically similar, phthalic and terephthalic acid differ substantially in topology. The presence of the two –COOH groups on opposite sides on the benzene moiety, beside making the intramolecular utilization of hydrogen bond donor and acceptor sites, impossible renders the terephthalate building block more elongated that the phthalate unit. This difference in shape is well reflected in the packing patterns, in which the $[C_6H_4\text{-}1,4\text{-}(COO)_2]^{2-}$ unit can take part.

The species $\{[(\eta^5\text{-}C_5H_5)_2Co]^+\}_4\{[C_6H_4(COOH)(COO)]^-\}_2[C_6H_4(COO)_2]^{2-}\cdot 4H_2O$ **V** is obtained when cobalticinium hydroxide and $[C_6H_4\text{-}1,2\text{-}(COOH)_2]$ are

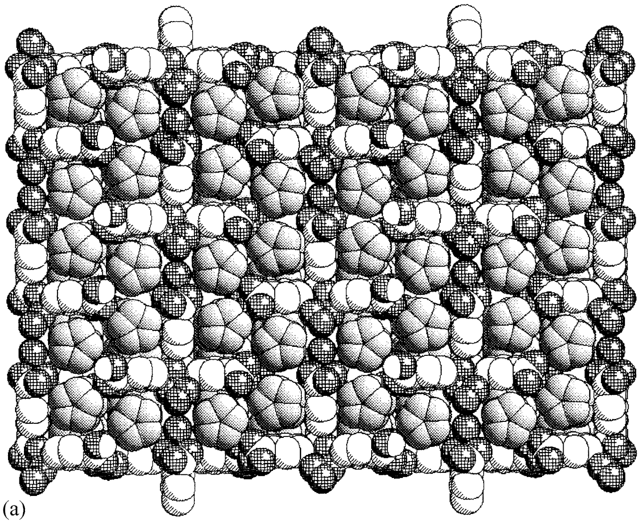
(a)

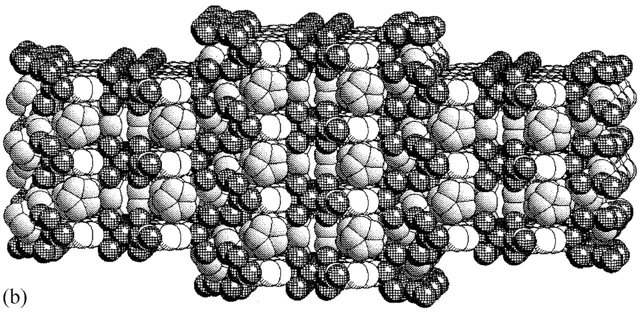
(b)

Fig. 3. (a) Space filling representation of the brick-wall type anionic organic superstructure present in crystalline **V** the cations are arranged in pairs of columns along the *c*-axis. (b) The channels are delimited on both sides only by water molecules and above and below by the terephthalate anions in **VII**. H_{cation} atoms omitted for clarity.

reacted in stoichiometric ratio 1:1. The crystal architecture recalls a brick wall, with large rectangular channels occupied by pairs of columns of $[(\eta^5\text{-}C_5H_5)_2Co]^+$ cations (see Fig. 3a). **V** contains two well distinct building blocks resulting from complete and partial deprotonation of $[C_6H_4\text{-}1,2\text{-}(COOH)_2]$, which plays different structural roles.

The two hydrogen bond arrangements in **V** represent two 'options' for phthalic acid. A third one is seen with the structure of $[(\eta^6\text{-}C_6H_6)_2Cr]^+\{[C_6H_4\text{-}(COOH)(COO)]^-[C_6H_4(COOH)_2]\}$ **VI**, which contains chains formed by an alternation of mono-deprotonated anions and of neutral $[C_6H_4\text{-}1,2\text{-}(COOH)_2]$ acid molecules, the –OH group of the $[C_6H_4\text{-}1,2\text{-}(COOH)(COO)]^-$ anion being used in intramolecular hydrogen bonding.

An example of hydrogen bonded network with participation of water molecules is offered by crystalline $\{[(\eta^5\text{-}C_5H_5)_2Co]^+\}_2[C_6H_4(COO)_2]^{2-}\cdot 6H_2O$ **VII**. This compound is constituted of $[C_6H_4(COO)_2]^{2-}$ anions, resulting from complete deprotonation of the $[C_6H_4(COOH)_2]$ acid, joined by hydrogen bonds with the six water molecules for formula unit. The water bridged $[C_6H_4(COO)_2]^{2-}$ system forms a fascinating anionic superstructure (see Fig. 3b) constituted of large, almost rectangular, channels delimited on the left and right sides only by water molecules, and above and below by the terephthalate anions. The large channeled structure accommodates the $[(\eta^5\text{-}C_5H_5)_2Co]^+$ cations.

3.4. Honeycomb aggregation

The organic acids D,L- and L-tartaric acid ($HO_2CCH(OH)\text{-}CH(OH)CO_2H$) have been utilized to generate honeycomb-type organic frameworks, encapsulating the organometallic cation $[(\eta^5\text{-}C_5H_5)_2Co]^+$.

The cobalticinium cation in crystalline **VIII** is encapsulated within an organic honeycomb-framework (see Fig. 4a) of stoichiometry $\{[(\text{D,L-}HO_2CCH(OH)CH(OH)CO_2)(\text{D,L-}HO_2CCH(OH)CH(OH)CO_2H)]^-\}_n$, generated by the aggregation of supramolecular monoanions $[(\text{D,L-}HO_2CCH(OH)\text{-}CH(OH)CO_2)(\text{D,L-}HO_2CCH(OH)CH(OH)CO_2H)]^-$ formed as a consequence of the loss of one proton every two tartaric acid molecules. The tartaric acid dimers are characterized by the presence of a strong –C(O)O–H···O(O)C– hydrogen bond (2.434(1) Å) between the two units, and are linked in the honeycomb framework via O–H···O bonds involving the two *external* carboxyl groups and the hydroxyl groups. The imbalance between the number of –OH and C=O acceptor sites and the number of 'conventional' donors (four –OH groups out of five participate in intramolecular –O–H···O bonds) is likely to be the driving force towards aggregation around the $[(\eta^5\text{-}C_5H_5)_2Co]^+$ cations. The interaction between the supramolecular anionic network and the cations occurs via $C\text{–}H^{(+)}\cdots O^{(-)}$ hydrogen bonds between the *staggered* cyclopentadienyl ligands of the cations and the –CO and the –OH groups of the anionic framework.

With this strategy it is relatively easy to obtain chiral *homo-ionic* networks. It is sufficient to use enantiomerically pure acids, such as L-tartaric acid, in the construction of the organic frameworks. When $\text{L-}(HO_2CCH(OH)CH(OH)\text{-}CO_2H)$ is employed, the chiral crystal $[(\eta^5\text{-}C_5H_5)_2Co]^+[(\text{L-}HO_2CCH(OH)CH(OH)CO_2)]^-$ **IX** is, in fact, obtained. The architecture is based on a 3D organic *super*-anion similar to that described above for **VIII**. The honeycomb-type structure (see Fig. 4b) is constituted of two types of squared-walls channels. The two channels differ in size and accommodate two crystallographically independent cobalticinium cations. In terms of hydrogen bonds the following observations can be made:

i) The two independent $[(\text{L-}HO_2CCH(OH)CH(OH)CO_2)]^-$ ions form strong negatively charge-assisted $O\text{–}H\cdots O^-$ hydrogen bonds of the type discussed above for **VIII**, generating parallel chains extending along the *c*-axis.
ii) The inter-chain link is provided here by –OH···O=C hydrogen bonds with the carbonyl groups that do not participate in the chain construction (O(H)···O 2.847(10) and 2.925(10) Å).

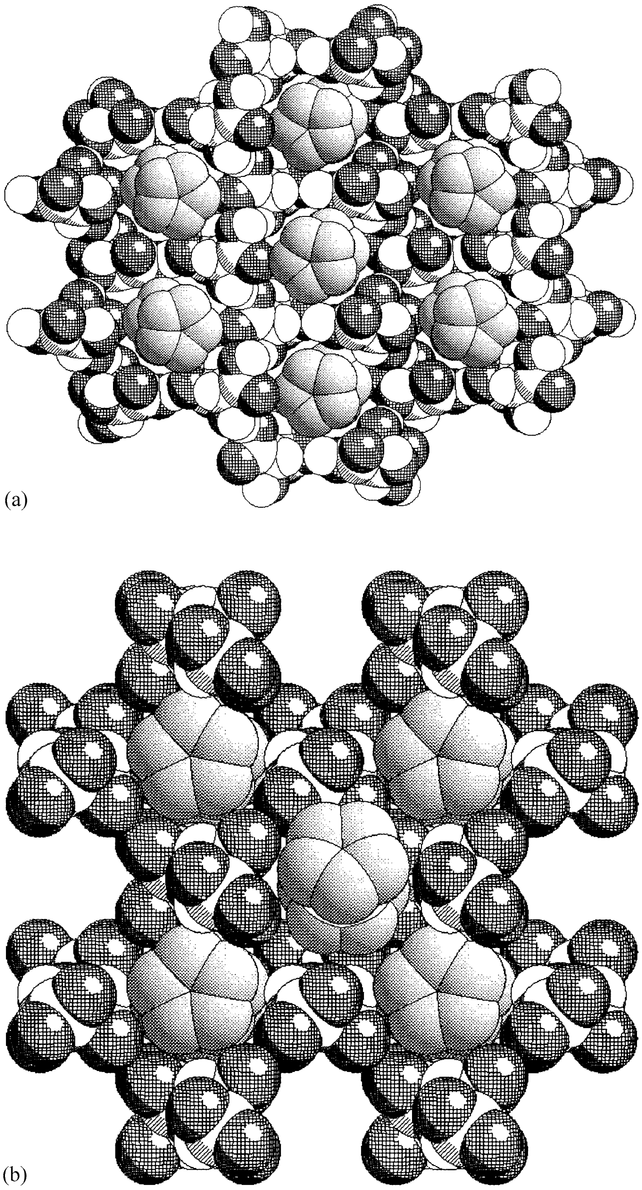

Fig. 4. (a) Space-filling representation of the anionic honeycomb framework formed by the [(D,L-$HO_2CCH(OH)CH(OH)CO_2$)(D,L-$HO_2CCH(OH)CH(OH)CO_2H$)]$^-$units in crystalline **VIII**. The cobalticinium cations pile inside the channels extending along the *a*-axis; cation H atoms are omitted for clarity. (b) Space-filling representation of the L-tartaric acid framework in crystalline **IX**. The cobalticinium cations pile inside the channels extending along the *c*-axis; H atoms omitted for clarity.

iii) An alternative way to look at the crystal architecture is to observe how the inter-chain links generate spirals (see Fig. 5), formed of an alternation of the two independent [(L-$HO_2CCH(OH)CH(OH)CO_2$)]$^-$ ions. The spirals are interwoven to form the channels and wrap around the cobalticinium cations.

iv) The interaction between the anionic superstructure and the encapsulated organometallic complex is again provided by C–H$\cdots$O hydrogen bonds.

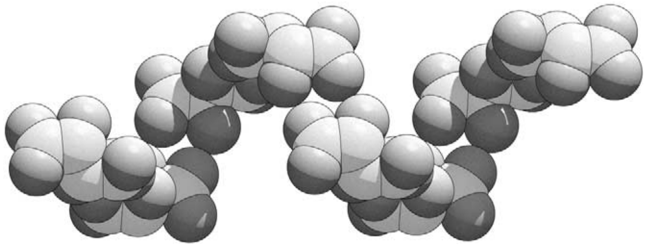

Fig. 5. A spiral of hydrogen bonded L-tartaric acid ions in crystalline **IX**. The spirals are interwoven to form the channels shown in Fig. 4b. H atoms omitted for clarity.

3.5. *Interpenetration and folding*

Trimesic acid, [C_6H_3-1,3,5-$(CO_2H)_3$], has been used to engineer crystals via negatively charged O–H$\cdots$O$^{(-)}$ and charge-assisted C–H$^{\delta+}\cdots$O$^{\delta-}$ hydrogen bonds upon reaction with [$(\eta^5\text{-}C_5H_5)_2Co$][OH], yielding [$(\eta^5\text{-}C_5H_5)_2Co$]$^+$-{[$C_6H_3(COOH)_3$][$C_6H_3(COOH)_2(COO)$]}$^-\cdot 2H_2O$, **X**. The salient structural features of crystalline **X** can be summarized as follows:

(1) There are two units derived from trimesic acid forming a dimeric superanion of formula {[$C_6H_3(COOH)_3$][$C_6H_3(COOH)_2(COO)$]}$^-$ from which only one acidic proton has been removed. The superanion is held together by a strong negative hydrogen bond between one –COOH system of one neutral acid molecule and the deprotonated –COO unit from a anionic [$C_6H_3(COOH)_2(COO)$]$^-$ system (see Fig. 6a).

(2) The water molecules bridge pairs of –COOH units and form 10-atom rings via insertion of one –OH group within the carboxylic ring, while the other –OH group of the same water molecules links the free oxygen atoms on the deprotonated inter-trimesic –COO–H–OOC– system, thus propagating the structure in the 3D by expanding to layers above and below the reference plane (see Fig. 6b). The benzene rings lie flat onto the next layer at a graphitic distance of 3.30 Å.

3.6. *Hinged folding and embracing*

Analogously to the case of **IX**, (*R*)-(+)-1,1′-bi-2-naphthol [(*R*)-(+)-($HOC_{10}H_6C_{10}H_6OH$)] has been used as a chiral building block in the construction of chiral organic–organometallic crystals. The reaction of the neutral molecule with [$(\eta^5\text{-}C_5H_5)_2Co$] in ether yields the supramolecular salts [$(\eta^5\text{-}C_5H_5)_2Co$][(*R*)-(+)-($HOC_{10}H_6C_{10}H_6O$)]·[(*R*)-(+)-($HOC_{10}H_6C_{10}H_6OH$)], **XI**, and [$(\eta^5\text{-}C_5H_5)_2Co$][(*R*)-(+)-($HOC_{10}H_6C_{10}H_6O$)]·[(*R*)-(+)-($HOC_{10}H_6C_{10}H_6OH$)]$_{0.5}$, **XII** depending on the stoichiometric ratios between the binaphthol and the organometallic sandwich compound. Molecular aggregation is achieved via a combination of neutral and charge-assisted O–H$\cdots$O bonds between the binaphthol and binaphtholate components, and via weaker interactions of the C–H$\cdots$O and C–H$\cdots\pi$ types involv-

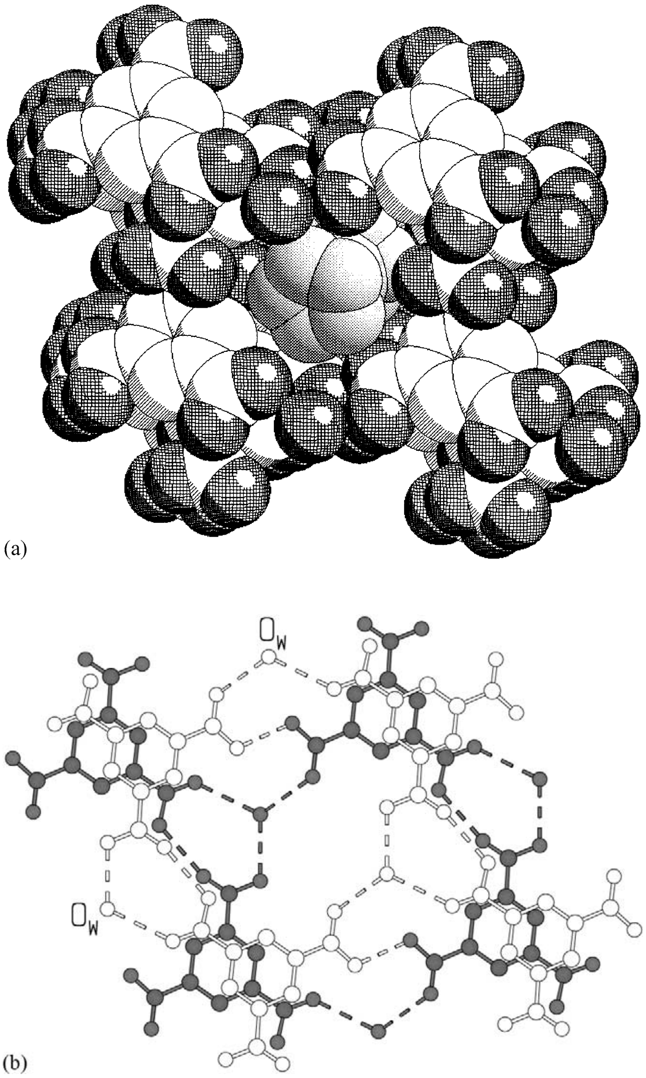

Fig. 6. Space filling representation of the anionic organic superstructure folding around the cobalticinium cation in crystalline **X** (a). The hydrogen bonding pattern involving anions and water molecules in crystalline **X** (b).

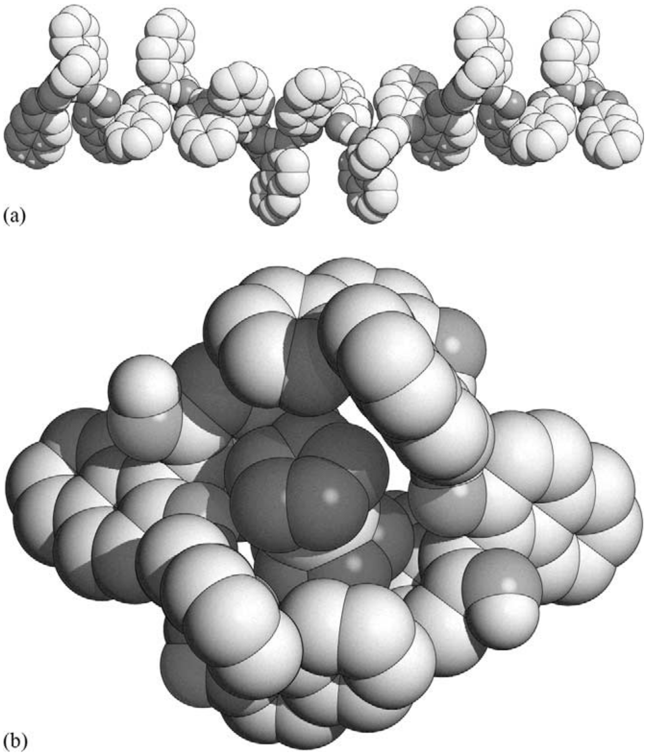

Fig. 7. Space filling representation of the chain in crystalline **XI**, formed by the neutral spacer and the anion (a). A space filling representation of the cation encapsulated by two binaphthol and two binaphtholate units (b). Only $H_{(OH)}$ atoms shown for clarity.

ing the cation $[(\eta^5\text{-}C_5H_5)_2Co]^+$. The same reaction with racemic 1,1′-bi-2-naphthol in ether followed by recrystallization from nitromethane yields the solvate species $[(\eta^5\text{-}C_5H_5)_2Co^{III}][(R,S)\text{-}(HOC_{10}H_6C_{10}H_6O)]\cdot[(R,S)\text{-}(HOC_{10}H_6C_{10}H_6OH)]\ [MeNO_2]_{1.5}$.

The main difference between **XI** and **XII** arises from the fact that compound **XI** contains one neutral molecule and one mono-deprotonated unit, while crystalline **XII** contains half neutral molecule per anionic unit. In **XI** the neutral molecules act as bridges between mono-anions, thus forming a chain system in which anions and neutral molecules alternate (see Fig. 7a), as observed before for **I**. The O–H$\cdots$O hydrogen bonds along the chain are of two types: the intermolecular O–H$\cdots$O$^{(-)}$ bond between the neutral spacer and the anion (2.667(7) and 2.612(7) Å, respectively), and the intramolecular hydrogen bond between the –OH group of the anion and the deprotonated oxygen atom (2.427(7) Å). Because of the enantiomerically pure nature of the component, the chain is chiral as in the case of L-tartaric acid (see Figs. 5 and 7a).

The interaction between the neutral-anionic chain and the cations is based on charge-assisted C–H$\cdots$O hydrogen bonds as well as on C–H$\cdots\pi$ interactions. The cations lie nestled between the wings of pairs of binaphthol molecules; where two chains come together the cation becomes totally encapsulated by a total of two binaphthol molecules and two binaphtholate anions (one each from each hydrogen-bonded chain), as shown in Fig. 7b.

The binaphthol molecule in compound **XII**, rather than forming infinite chains, acts as a bridge between two mono-deprotonated anions. The resulting trimeric unit embraces two cations, as shown in Fig. 8.

3.7. *Partial conclusions*

The design criteria employed above (*strategy 1*) can be summarized as follows:

(i) Confinement of all (or most) strong donor/acceptor hydrogen bonding groups on the organic (usually anionic) network and exclusion of the organometallic fragments (usually cationic) leads to selective self-assembling of the organic fragments in complex superstructures, whose topology depends on the size, shape and number and geometry of the –OH/–COOH/COO$^{(-)}$ groups;

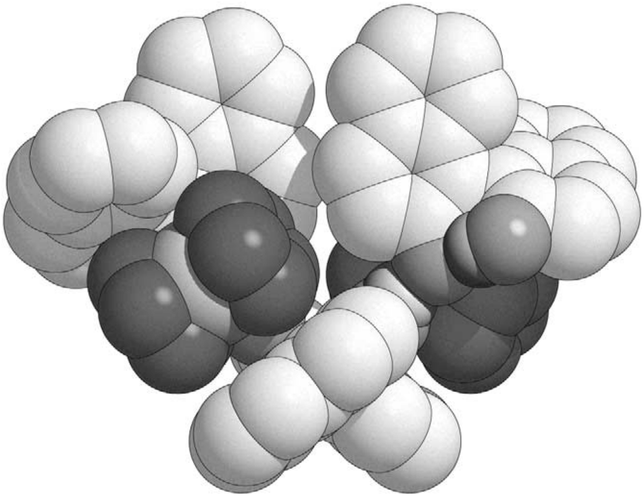

Fig. 8. Space filling representation showing how the supramolecular dianions in **XII** *embrace* two cations, optimizing the C–H···π interactions.

(ii) The large number of polarized C–H$^{(\delta+)}$ groups carried by arene and cyclopentadienyl ligands, belonging to organometallic cations, allows one to fully exploit the 'free' hydrogen bonding acceptor sites on the organic framework, and to stabilize the superstructures via C–H$^{(\delta+)}\cdots$O$^{(-)}$ interactions.

In terms of building block shape we have seen that, when the small and tubular hydrogen oxalate anion is used, it is possible to *force* the paramagnetic sandwich cations to closer contact without anion intercalation. This 1D arrangement has been shown to lead to cooperative magnetic properties. Linear arrangements of the type C$^{(+)}$–C$^{(+)}$–C$^{(+)}$–C$^{(+)}$ surrounded by chains of A$^{(-)}$–A$^{(-)}$–A$^{(-)}$–A$^{(-)}$ anions, or intercalated between layers of anions, are not easily obtained, because of the tendency of the ions of a given sign to be surrounded by ions of opposite sign. This is the main motivation for using small anions. Earlier studies of crystals containing flat radical anions [29d], such as tetracyanoethylene (TCNE$^{\bullet-}$), tetracyano-*p*-quinodimethane (TCNQ$^{\bullet-}$) or other similar anions, and radical cations such as [Fe(η^5-C$_5$Me$_5$)$_2$]$^+$, as well as other sandwich cations (e.g. [Cr(η^6-C$_6$Me$_x$H$_{6-x}$)$_2$]$^+$), have led to the formulation of the *linear-chain paradigm*, which postulates the formation of sequences of the type A$^{(-)}$–C$^{(+)}$–A$^{(-)}$–C$^{(+)}$ between radical anions and cations in crystals.

4. Hydrogen bonded networks formed by organometallic sandwich units

In this section we describe hydrogen bonded networks formed by functionalized organometallic molecules, according mainly to *strategy 2*. Contrary to the cases shown in the preceding section, the organometallic compounds described in this section *do take part* in the hydrogen bonding network. Strategy 2 thus represents a viable route to the formation of hybrid organic–organometallic and organometallic–organometallic structures. Some examples are summarized in Table 3.

The description follows a different logic than the one adopted in the previous section, where the attention was focused on the change in network topology as a function of the size, shape and number of donor/acceptor groups. The combination of oxidation state and charge of the complex, in fact, allows the utilization of organometallic molecules not only as neutral building blocks, but also as cationic and anionic units.

4.1. Hybrid organic–organometallic crystals

The organometallic dicarboxylic acid [(η^5-C$_5$H$_4$COOH)$_2$Fe] **XIII** has been used as hydrogen bonding building block in the preparation of hybrid organic–organometallic and of organometallic–organometallic crystal architectures. It should be mentioned, on passing, that **XIII** is known in two polymorphic modifications [30] that differ in the relative orientation of the hydrogen bonded molecular pairs (Fig. 9). Even though polymorphism is an important issue

Table 3
Hybrid organic–organometallic, organometallic–organometallic networks

Organometallic acid	Counterion	Formula	**n**
Ferrocendicarboxylic [30]	–	[(η^5-C$_5$H$_4$COOH)$_2$ Fe^{II}]	**XIII**
Ferrocendicarboxylic [32]	[C$_8$H$_{16}$N$_4$]$^{2+}$	[C$_8$H$_{16}$N$_4$]$^{2+}${[(η^5-C$_5$H$_4$COOH)(η^5-C$_5$H$_4$COO)Fe]$_2$}$^{2-}$	**XIV**
Ferrocendicarboxylic [32]	[C$_{10}$H$_{20}$N$_4$]$^{2+}$	[C$_{10}$H$_{20}$N$_4$]$^{2+}${[(η^5-C$_5$H$_4$COOH)(η^5-C$_5$H$_4$COO)Fe]$_2$}$^{2-}$	**XV**
Ferrocendicarboxylic [33]	[(η^5-C$_5$H$_5$)$_2$Co]$^+$	[(η^5-C$_5$H$_5$)$_2$Co]$^+$[(η^5-C$_5$H$_4$COOH)(η^5-C$_5$H$_4$COO)Fe]$^-$	**XVI**
Ferrocendicarboxylic [33]	[(η^5-C$_5$H$_5$)$_2$Co]$^+$	[(η^5-C$_5$H$_5$)$_2$Co]$^+$[(η^5-C$_5$H$_4$COOH)(η^5-C$_5$H$_4$COO)Fe]$^-$·H$_2$O	**XVII**
Ferrocendicarboxylic [33]	[(η^6-C$_6$H$_6$)$_2$Cr]$^+$	{[(η^6-C$_6$H$_6$)$_2$Cr]$^+$}$_2${[(η^5-C$_5$H$_4$COOH)(η^5-C$_5$H$_4$COO)Fe]$_2$ [(η^5-C$_5$H$_4$COOH)$_2$Fe]}^{2}	**XVIII**
Ferrocendicarboxylic [33]	[(η^6-C$_6$H$_6$)$_2$Cr]$^+$	[(η^6-C$_6$H$_6$)$_2$Cr]$^+${[(η^5-C$_5$H$_4$COOH)(η^5-C$_5$H$_4$COO)F]}$^-$·H$_2$O	**XIX**
Bis-benzene chromium dicarboxylic [34]	–	[(η^6-C$_6$H$_5$COOH)$_2$Cr^0]	**XX**
Bis-benzene chromium dicarboxylic [34]	[PF$_6$$^-$]	[(η^6-C$_6$H$_5$COOH)$_2$Cr^I][PF$_6$]	**XXI**
Bis-benzene chromium dicarboxylic [34]	–	[(η^6-C$_6$H$_5$COOH)(η^6-C$_6$H$_5$COO)Cr^I]	**XXII**
Cobalticinium dicarboxylic [35]	Several	[(η^5-C$_5$H$_4$COOH)$_2$Co^{III}]$^+$	**XXIII**
Cobalticinium dicarboxylic [35]	–	[(η^5-C$_5$H$_4$COOH)(η^5-C$_5$H$_4$COO)Co^{III}]	**XXIV**
Cobalticinium dicarboxylic [35]	[NH$_4$$^+$]	[(η^5-C$_5$H$_4$COO)$_2$Co^{III}]$^-$	**XXV**

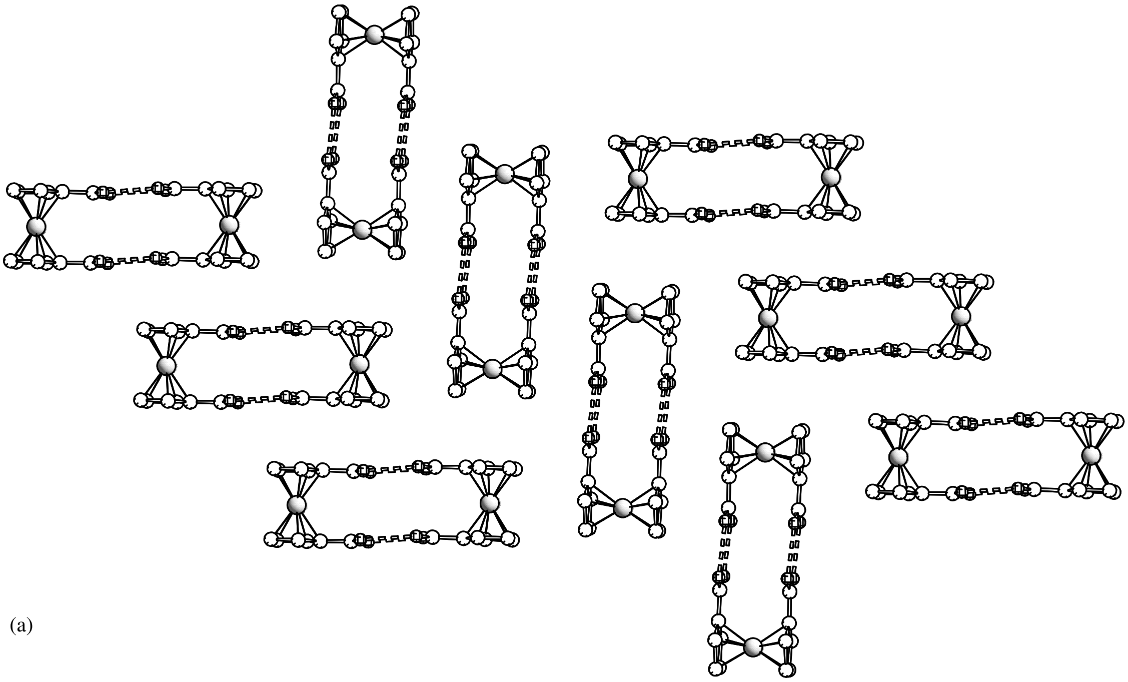

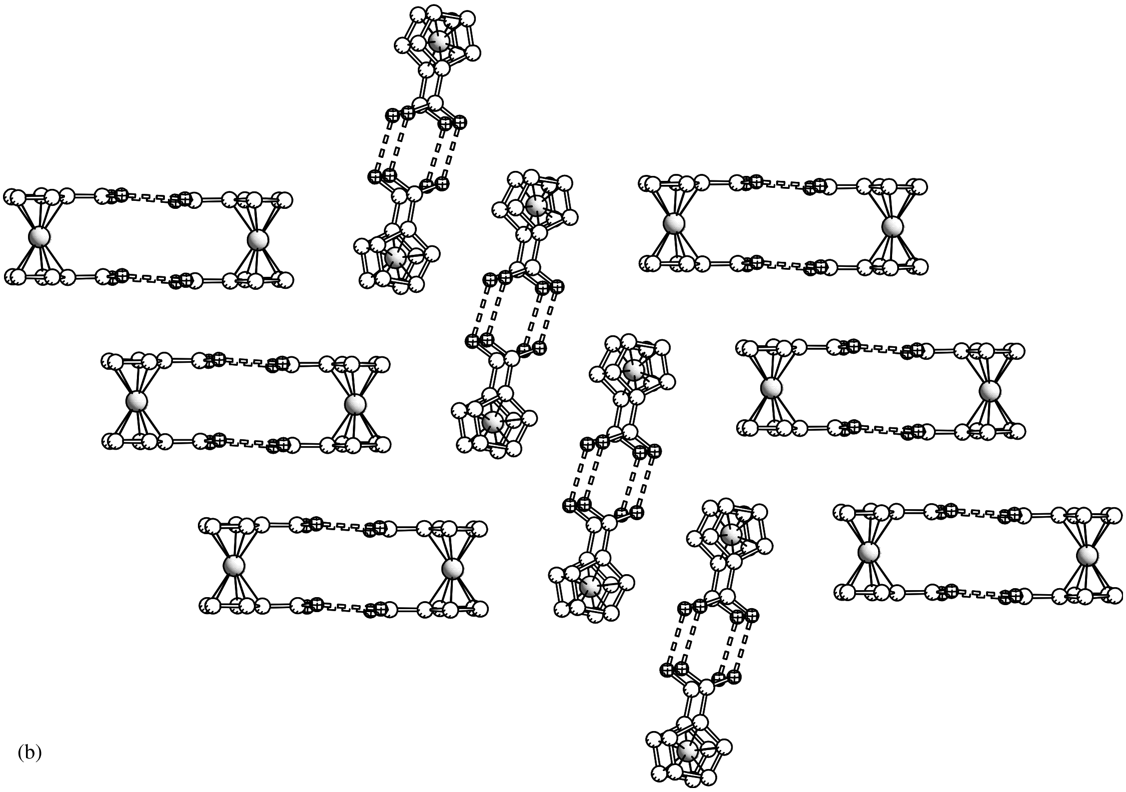

Fig. 9. Comparison of the monoclinic (a) and triclinic (b) forms of crystalline **XIII**. H atoms are omitted for clarity.

when discussing hydrogen bonding networks, the subject will be touched only marginally in the following. The reader is addressed to Ref. [31] for relevant literature entries.

The compounds $[C_8H_{16}N_4]^{2+}\{[(\eta^5\text{-}C_5H_4COOH)(\eta^5\text{-}C_5H_4COO)Fe]_2\}^{2-}$, **XIV**, and $[C_{10}H_{20}N_4]^{2+}$ $\{[(\eta^5\text{-}C_5H_4COOH)(\eta^5\text{-}C_5H_4COO)Fe]_2\}^{2-}$, **XV**, have been obtained by reacting $[(\eta^5\text{-}C_5H_4COOH)_2Fe]$ with the bis-amidines $[C_8H_{14}N_4]$, and $[C_{10}H_{18}N_4]$, respectively, [32]. The self-assembly between mono- and di-deprotonated acids and the protonated cations is controlled by the stoichiometric ratio and by the choice of solvent. An acid:base stoichiometric ratio of 2:1 allows partial deprotonation of the acid, thus affording species that show the simultaneous presence of *homo-ionic* $O–H^{(-)}\cdots O^{(-)}$ and *hetero-ionic* $N–H^{(+)}\cdots O^{(-)}$ interactions, but do not contain solvent molecules. This is an important, albeit simple, stoichiometric control on the superstructure of the crystalline materials. If –COOH groups are 'left' on the anion, there is competition in hydrogen bond formation between the $–N–H^{(+)}$ donor (favored by the positive ionic charge carried by the bis-amidine cations) and the –O–H donor, which generally forms O–H···O bonds that are stronger than neutral N–H···O.

The absence of solvent molecules in both **XIV** and **XV** indicates that the number of donor –O–H and N–H groups, resulting from partial deprotonation of the diacid and protonation of the base, is sufficient to satisfy all acceptor sites with strong interactions. Crystalline **XIV** can be described as formed by *homo-ionic* chains of anionic acidates interacting with the bis-amidines in *dihapto* mode. Fig. 10a shows a 2D network in **XIV**: the ionic arrangement can alternatively be described as composed of chains of $O–H^{(-)}\cdots O^{(-)}$ interacting $[(\eta^5\text{-}C_5H_4COOH)(\eta^5\text{-}C_5H_4COO)Fe]^-$ anions joined by bis-amidines bridges, or as trimeric units, each formed by a bis-amidine dication hooking together two ferrocene monoacidates. The hydrogen bonds between the bis-amidine and the carboxylate groups are N(H)···O 2.832(2) and 2.799(2) Å, respectively. The O–H···O interaction along the acidate chain is short (2.546(2) Å) and comparable in length to the one present in crystalline **XV**. Indeed, crystalline **XV** can also be described as formed by chains of mono-deprotonated $[(\eta^5\text{-}C_5H_4COOH)(\eta^5\text{-}C_5H_4COO)Fe]^-$ anions interacting with the protonated bis-amidine $[C_{10}H_{20}N_4]^{2+}$ in *dihapto* mode (see Fig. 10). The N···O distances of the charged assisted hydrogen bonds [N(–H)···O 2.724(2) and 2.764(2) Å] are comparable to the values discussed before. As in **XIV** the organometallic anions are linked via O–H···O interactions (O···O distance 2.542(2) Å).

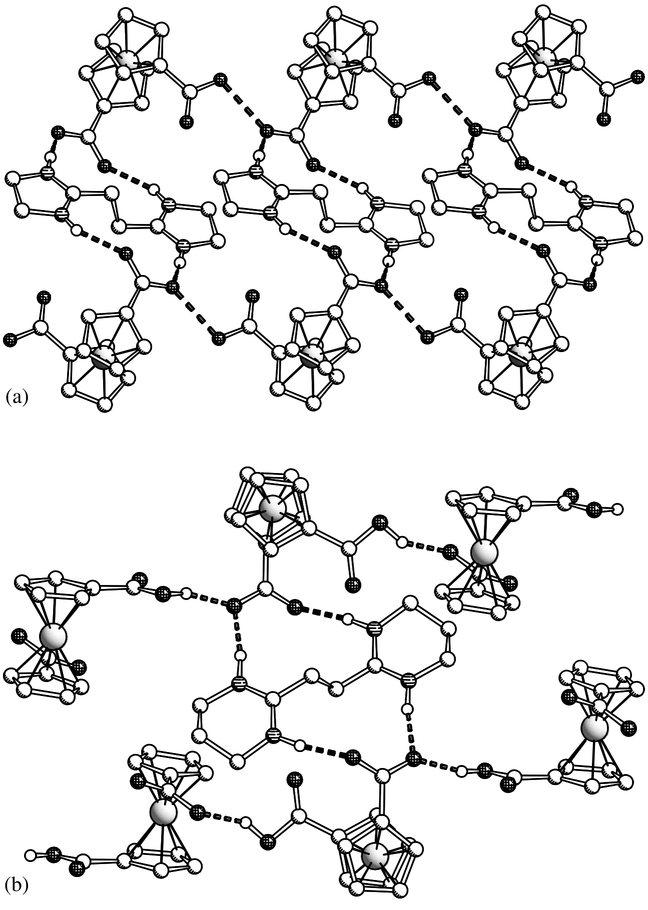

Fig. 10. (a) The ribbons formed by two chains of $[(\eta^5\text{-}C_5H_4COOH)\text{-}(\eta^5\text{-}C_5H_4COO)Fe]^-$ interacting with the dication $[C_8H_{16}N_4]^{2+}$ via charge-assisted hydrogen bonds in **XIV**. (b) Portion of the 3D network, formed by the monoanion $[(\eta^5\text{-}C_5H_4COOH)(\eta^5\text{-}C_5H_4COO)Fe]^-$ chains interacting with the dication $[C_{10}H_{20}N_4]^{2+}$ in **XV**. Only $H_{(NH)}$ and $H_{(COOH)}$ atoms shown for clarity.

4.2. Mixed-metal hydrogen bonded networks

The dicarboxylic organometallic acid $[(\eta^5\text{-}C_5H_4COOH)_2Fe]$ **XIII** has been used to produce a series of novel mixed-metal, mixed-valent crystalline materials by exploiting a modification of the reaction sequence discussed above. The reaction proceeds stepwise according to the following sequence: (i) oxidation in the air of THF solutions of $[(\eta^5\text{-}C_5H_5)_2Co]$ and $[(\eta^6\text{-}C_6H_6)_2Cr]$ and consequent reduction of O_2 to the strongly basic anion $O_2{}^-$; (ii) deprotonation of **XIII** to yield the anion $\mathbf{XIII}^-$ (or $\mathbf{XIII}^{2-}$); (iii) precipitation of the insoluble organometallic salts formed between the organometallic acidate and the diamagnetic cation $[(\eta^5\text{-}C_5H_5)_2Co]^+$ or the paramagnetic cation $[(\eta^6\text{-}C_6H_6)_2Cr]^+$. The materials $[(\eta^5\text{-}C_5H_5)_2Co]^+[(\eta^5\text{-}C_5H_4COOH)(\eta^5\text{-}C_5H_4COO)Fe]^-$ **XVI**, $[(\eta^5\text{-}C_5H_5)_2Co]^+[(\eta^5\text{-}C_5H_4COOH)\ (\eta^5\text{-}C_5H_4COO)Fe]^-\cdot H_2O$ **XVII**, $\{[(\eta^6\text{-}C_6H_6)_2Cr]^+\}_2\{[(\eta^5\text{-}C_5H_4COOH)(\eta^5\text{-}C_5H_4COO)Fe]_2[(\eta^5\text{-}C_5H_4COOH)_2Fe]\}^{2-}$ **XVIII** and $[(\eta^6\text{-}C_6H_6)_2Cr]^+\{[(\eta^5\text{-}C_5H_4COOH)(\eta^5\text{-}C_5H_4COO)Fe\}^-\cdot H_2O$ **XIX** have been prepared and structurally characterized. The four species contain different electronic and spin metal centers: 18 electrons Fe^{II} and Co^{III} metal atoms are present in **XVI** and **XVII**, whereas 18-electrons Fe^{II} and paramagnetic 17 electrons Cr^{I} are present in **XVIII** and **XIX**. The crystalline edifices are held together by the complementary contribution of neutral O–H···O and/or negatively charged $O–H\cdots O^{(-)}$ hydrogen bonding interactions between the acid moieties and of *charge assisted* $C–H^{\delta+}\cdots O^{\delta-}$ bonds between cations and anions.

In crystalline **XVI** the $[(\eta^5\text{-}C_5H_4COOH)(\eta^5\text{-}C_5H_4COO)Fe]^-$ anions, derived from mono-deprotonation of the neutral acid, form chains via symmetric O···H···O interactions between ligands in *transoid* conformation (see Fig. 11a). Charge assisted $C–H^{\delta+}\cdots O^{\delta-}$ hydrogen bonds link then the cobalticinium cations to the

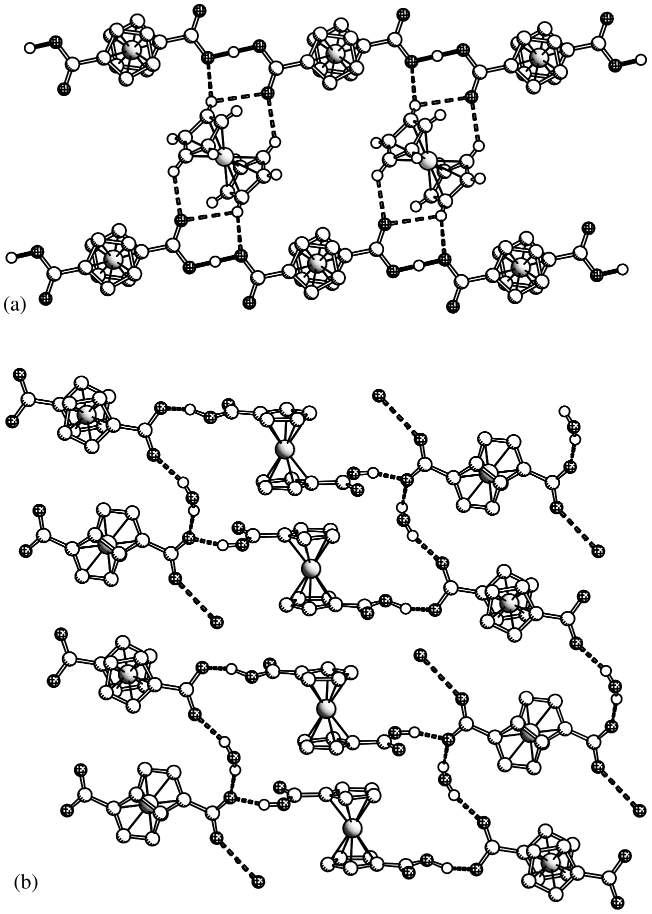

Fig. 11. (a) In crystalline **XVI** the $[(\eta^5\text{-}C_5H_4COOH)(\eta^5\text{-}C_5H_4COO)Fe]^-$ anions form parallel chains enclosing the $[(\eta^5\text{-}C_5H_5)_2Co]^+$ cations. (b) In crystalline **XVII** the $[(\eta^5\text{-}C_5H_4COOH)_2Fe]$ and $[(\eta^5\text{-}C_5H_4COO)_2Fe]^{2-}$ anions form chains via O–H···O hydrogen bonding interactions. Only experimentally located $H_{(OH)}$ atoms are shown.

$[(\eta^5\text{-}C_5H_4COOH)(\eta^5\text{-}C_5H_4COO)Fe]^-$ chains. The two sets of three $C\text{–}H^{\delta+}\cdots O^{\delta-}$ hydrogen bonds on both sides of the cations are directed towards the unused lone pairs on the carboxylic oxygen atoms.

Although the stoichiometry of compound **XVII** corresponds to the formula $[(\eta^5\text{-}C_5H_5)_2Co]^+[(\eta^5\text{-}C_5H_4COOH)\text{-}(\eta^5\text{-}C_5H_4COO)Fe]^-\cdot H_2O$, the distribution of –COOH groups indicates that the asymmetric unit is composed of one fully protonated ferrocenedicarboxylic acid $[(\eta^5\text{-}C_5H_4COOH)_2Fe]$ unit in general position and of two ‘half’ dianionic, i.e. completely deprotonated, $[(\eta^5\text{-}C_5H_4COO)_2Fe]^{2-}$ units, in addition to two cobalticinium cations and two water molecules. The assignment of neutral and anionic units to the ferrocene moieties is in agreement with the distribution of bond length within the carboxylic/carboxylate groups. The chains shown in Fig. 11b can be described as resulting from the neutral/dianion alternation, e.g. $\text{–}[(\eta^5\text{-}C_5H_4COO)_2Fe]^{2-}\text{–}[(\eta^5\text{-}C_5H_4COOH)_2Fe]\text{–}[(\eta^5\text{-}C_5H_4COOH)_2Fe]^{2-}\text{–}[(\eta^5\text{-}C_5H_4COOH)_2Fe]\text{–}$.

Similar alternations of anions and neutral molecules have been described above for compounds **I** and **VIII**. The O···O hydrogen bonding distances along the chains in **XVII** are 2.49(2), and 2.52(2) Å, i.e. slightly longer than in **XVI** (2.45(2) Å). It can be argued that the alternation of dianion and neutral molecules within the chains in **XVII** achieves the important result of decreasing the electrostatic repulsion between anionic species. A chain formed by mono-deprotonated ferrocenedicarboxylic acid as in **XVI** with respect to the chain $\text{–}[(\eta^5\text{-}C_5H_4COO)_2Fe]^{2-}\text{–}[(\eta^5\text{-}C_5H_4COOH)_2Fe]\text{–}[(\eta^5\text{-}C_5H_4COOH)_2Fe]^2\text{–}[(\eta^5\text{-}C_5H_4COOH)_2Fe]\text{–}$ in **XVII** possesses exactly the same *number of hydrogen bonds*, but should pay a larger electrostatic repulsion than in the latter, where the neutral molecule may act as a *neutral spacer* between the two anions. The balance must be subtle and the overall difference in energy not very large.

It has been recently shown that compound **XVII** can also be obtained by *grinding* solid **XVI** in the air, i.e. in the presence of aqueous vapor [33]. The identification of the compound has been possible by comparing the measured powder diffractogram with that calculated on the basis of the observed single crystal structure.

The ferrocene moieties in **XVII** also possess two different conformations: in projection the ligands in $\mathbf{XIII}^{2-}$ are *transoid*, with the C_5 ring *staggered*, while in the neutral **XIII** molecule the conformation can be described as *pseudo transoid*, with the C_5 rings *eclipsed* in projection. The dianions $\mathbf{XIII}^{2-}$ are tilted with respect to the molecule of **XIII** (see Fig. 11b), so as to allow formation of hydrogen bonds with the water molecules. The role of these molecules is clear to see, they act as bridges between the chains $\text{–}[(\eta^5\text{-}C_5H_4COO)_2Fe]^2\text{–}[(\eta^5\text{-}C_5H_4COOH)_2Fe]\text{–}[(\eta^5\text{-}C_5H_4COOH)_2Fe]^{2-}\text{–}[(\eta^5\text{-}C_5H_4COOH)_2Fe]\text{–}$, forming a 2D anionic layer structure ($O\cdots O_w$ distances 2.733, 2.814, 2.835(3) Å). The interaction between the supra-anionic network and the cobalticinium cations occurs via C–H···O hydrogen bonds between the *staggered* cyclopentadienyl ligands of the cations and the oxygen of the carboxylic/carboxylate group and the oxygen of the water.

The formula unit in crystalline **XVIII** contains one neutral molecule of **XIII** every two $\mathbf{XIII}^-$ anions. The neutral molecule acts as a bridge between hydrogen bonded dimers formed by two $\mathbf{XIII}^-$ anions. In a way **XVIII** recalls the situation observed for **XVII** with the neutral molecule acting as a buffer (a spacer) between the anionic units (see Fig. 12a). The neutral-anion $O\text{–}H\cdots O^{(-)}$ hydrogen bond is of the same length as that between the two mono-anions (2.570(5) versus 2.569(5) Å). All ‘unused’ acceptor sites on the O-atoms are directed outwards along the chain to attain the maximum number of $C\text{–}H^{\delta+}\cdots O^{\delta-}$ interactions with the $[(\eta^6\text{-}C_6H_6)_2Cr]^+$ cations. These values are again indicative of a substantial electrostatic reinforcement of the weak bonds. The presence of pairs of $[(\eta^6\text{-}C_6H_6)_2Cr]^+$ cations in the packing of **XVIII** is noteworthy.

Crystalline **XIX** presents two mono-deprotonated $\mathbf{XIII}^-$ units in general position, two $[(\eta^6\text{-}C_6H_6)_2Cr]^+$ cations

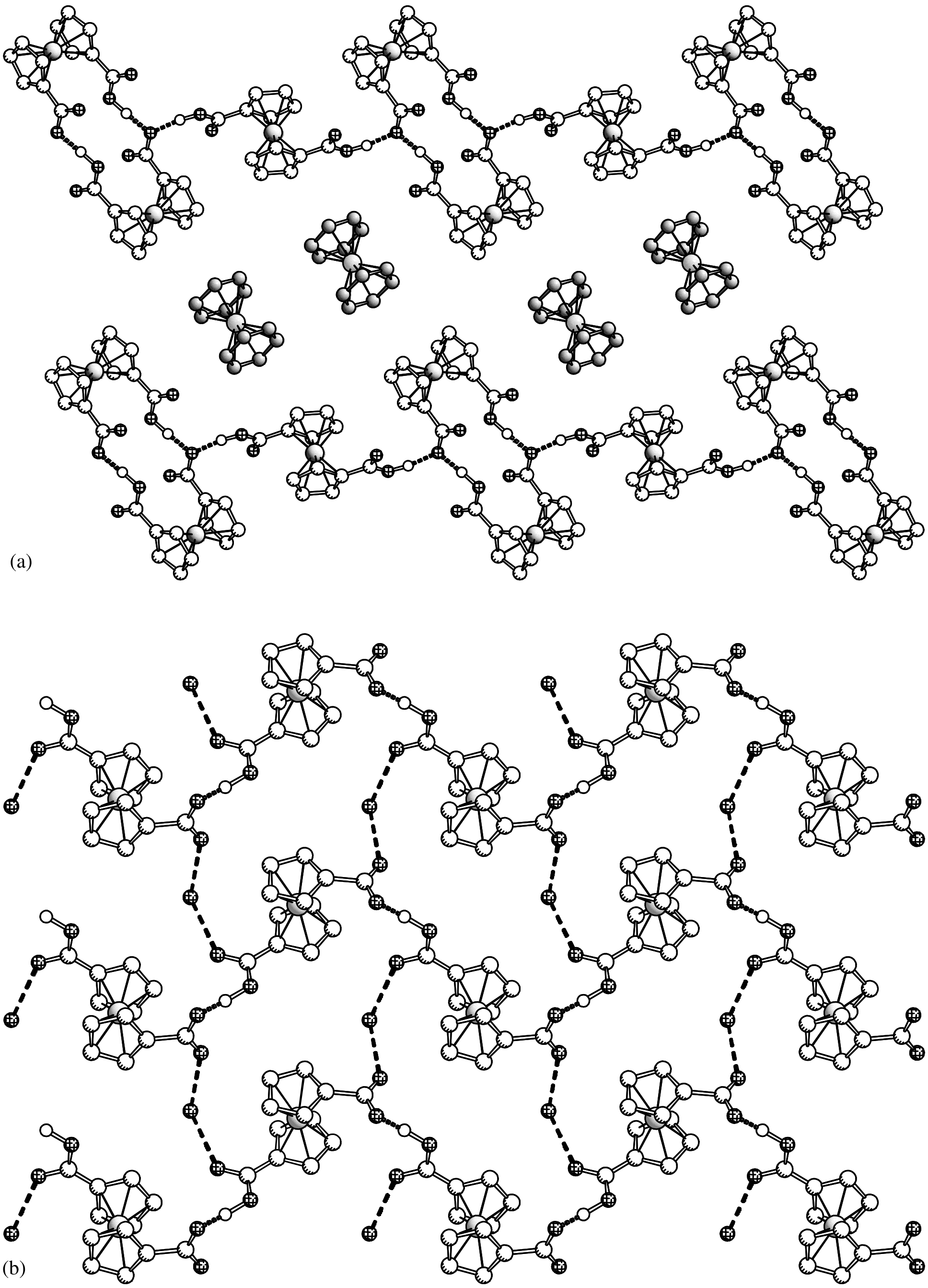

Fig. 12. (a) In crystalline **XVIII** the neutral **XIII** molecule acts as a bridge between hydrogen bonded dimers formed by two **XIII**$^{-}$ anions. There are two types of O–H···O hydrogen bonding interactions, those within the $\{[(\eta^5\text{-}C_5H_4COOH)(\eta^5\text{-}C_5H_4COO)Fe]_2\}^{2-}$ unit and those between these units and the neutral $[(\eta^5\text{-}C_5H_4COOH)_2Fe]$ spacer. (b) In crystalline **XIX** the **XIII**$^{-}$ anions form zigzag chains via O–H···O hydrogen bonding interactions. These chains are linked by water molecules, forming a layer on which the cations (not shown here) are located.

and two water molecules. The length of the two independent O–H···O$^{(-)}$ hydrogen bonding interactions is similar (2.461 and 2.438(3) Å) and comparable to the values commonly found in this type of *homo-ionic* hydrogen bonding interactions. The **XIII**$^{-}$ anions are in *pseudo-transoid* conformation with the C_5 ring *eclipsed* and form a zigzag chain. The water molecules act as bridges between the chains (O···O_w distances 2.747, 2.815, 2.821, 2.847(3) Å). It is worth noting that all oxygen atoms are involved in O–H···O hydrogen bonds, as shown in Fig. 12b. The interaction between the supramolecular anionic network and the cobalticinium cations occurs via charge assisted C–H$^{\delta+}$···O$^{\delta-}$ hydrogen bonding interactions, between the *staggered* cyclopentadienyl ligands of the cations and the oxygen of the carboxylic/carboxylate group and the oxygen of water.

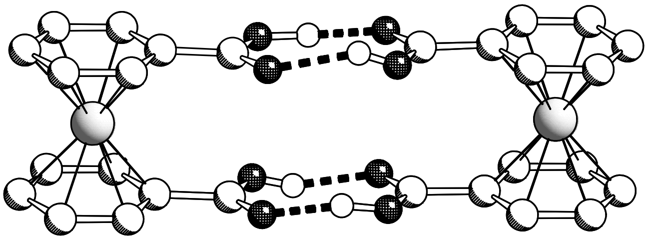

Fig. 13. Ball-and-stick representation of the dimer formed by molecules of **XX** in the solid state.

4.3. Neutral and cationic acids of [(η^6-$C_6H_5COOH)_2Cr$]

The ‘Cr-diacid family’ represents an interesting example of the potentials of organometallic molecules in supramolecular bonding. The neutral diamagnetic organometallic dicarboxylic acid [(η^6-$C_6H_5COOH)_2Cr$] **XX** is depicted in Fig. 13. While the neutral diacid molecule aggregates as hydrogen bonded dimers, analogous to that described above in the case of **XIII**, the oxidized form aggregates in *homo-ionic* chains, and the neutral zwitterionic form in hydrogen bonded dimers [34]. In fact, oxidation of **XX** by oxygen leads to formation of the paramagnetic dicarboxylic acid cation [(η^6-$C_6H_5COOH)_2Cr]^+$, **XXI**, which has been isolated as its $[PF_6]^-$ salt. The neutral zwitterionic form [(η^6-C_6H_5COOH)(η^6-C_6H_5COO)Cr], **XXII**, has been obtained in a co-crystal with $[NH_4][PF_6]$ upon treatment of the acid salt [(η^6-$C_6H_5COOH)_2Cr][PF_6]$ with ammonia.

Removal of protons from neutral **XX** leads to sequential formation of a monoanion and of a dianion, while deprotonation of **XXI** leads first to formation of the neutral sandwich zwitterion [(η^6-C_6H_5COOH)(η^6-$C_6H_5COO)Cr^I$] **XXII**, with one –COOH and one $–COO^{(-)}$ system. Further deprotonation of **XXII** leads to the dicarboxylate monoanion [(η^6-$C_6H_5COO)_2Cr]^-$, possessing two $–COO^{(-)}$ groups. Hence, the bis-benzene chromium system can be regarded as composed of a fundamental building block, namely ‘[(η^6-$C_6H_5COO)_2Cr$]’, which can participate, depending on the extent of protonation and on the metal atom oxidation state, in hydrogen bonding networks as a mono-cation, a neutral species, and as a mono- and di-anion unit.

It was mentioned above that, in the solid state, complex **XX** forms a dimer via a pair of typical hydrogen bonding rings involving the two –COOH groups of the acid. Twin intermolecular hydrogen bonding of the type shown by **XX** are not commonly observed with organic dicarboxylic acids, because dimer formation requires a degree of structural flexibility that cannot be afforded by molecules based on C–C σ-bonds. In fact, dicarboxylic organic acids tend to form chains in the solid state, rather than self-assemble in dimeric units. Compound **XX**, and all is congeners, can instead *rotate* around the coordination axis of the carbocyclic ligands, to yield the eclipsed conformation of the –COOH groups required for the formation of the dimer. The oxidized form **XXI** is known in two crystalline polymorphic modifications, a monoclinic form α and a triclinic form β. Both polymorphs contain cationic chains placed side-by-side and forming a step-ladder superstructure with the $[PF_6]^-$ anions accommodated between the steps, as shown in Fig. 14. The O···O separations differ slightly in the two crystals, 2.629(2) and 2.634(2) in the α form and 2.618(4) Å in the β form.

The zwitterionic form of compound **XXI**, namely [(η^6-C_6H_5COOH)(η^6-C_6H_5COO)Cr], **XXII**, was obtained as a co-crystal with ammonium hexafluorophosphate. The zwitterion forms dimers joined together by two short hydrogen bonding interactions (2.477(2) Å), as shown in Fig. 15. It should be stressed that the difference between the *neutral* dimer formed by **XX** and the *neutral* dimer formed by **XXII** is not trivial: **XX** and **XXII** have metal atoms in different oxidation states, beside involving twice as many hydrogen bonding interactions in the dimer formation.

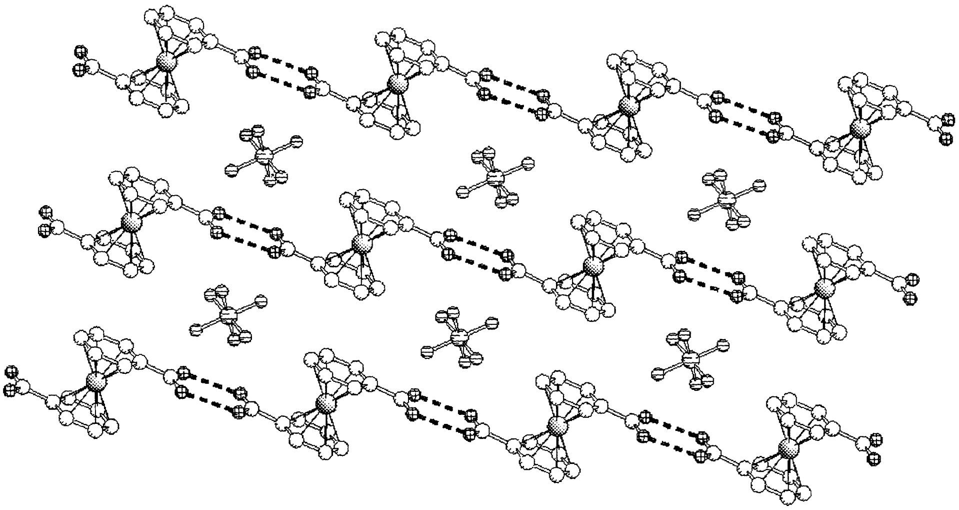

Fig. 14. The step-ladder superstructure formed by the hydrogen bonded cationic chains in both α and β forms of crystalline **XXI**, with the $[PF_6]^-$ anions accommodated between the steps. H atoms not shown for clarity.

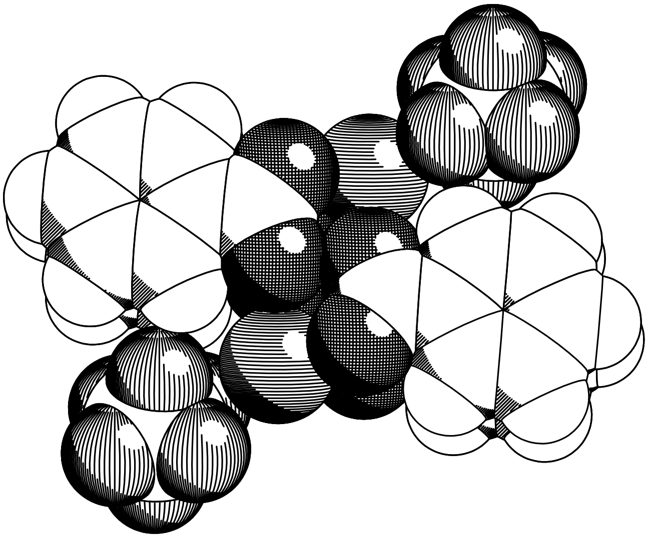

Fig. 15. Space filling representation showing how the $[NH_4]^+$ cations (represented here as spheres) in crystalline **XXII** $[NH_4][PF_6]$ interact with the zwitterionic dimers of **XXII** and the $[PF_6]^-$ anions.

4.4. *Zwittwerionic and cationic acids of $[(\eta^5\text{-}C_5H_4COOH)_2Co]^+$*

The water soluble dicarboxylic cationic acid $[(\eta^5\text{-}C_5H_4\text{-}COOH)_2Co]^+$, **XXIII**, has proven to be an extremely versatile building block for the construction of hydrogen bonded networks. What is more, the networks formed by the complex in cationic or zwitterionic form can be made *react* in solid–solid and solid–gas processes (see below).

Removal of one proton from **XXIII** leads to formation of the neutral zwitterion $[(\eta^5\text{-}C_5H_4COOH)(\eta^5\text{-}C_5H_4COO)Co]$ **XXIV**, while further deprotonation leads to formation of the dicarboxylate monoanion $[(\eta^5\text{-}C_5H_4COO)_2Co]^-$ **XXV**. The cationic form **XXIII** has been characterized in different crystalline salts, namely $[PF_6]^-$, Cl^-, as well as in its co-crystal with urea, and with the zwitterionic form **XXIV** in $\{[(\eta^5\text{-}C_5H_4COOH)(\eta^5\text{-}C_5H_4COO)Co][(\eta^5\text{-}C_5H_4COOH)_2Co]\}[PF_6]$. The neutral, paramagnetic, form $[(\eta^5\text{-}C_5H_4COOH)_2Co^{II}]$ has not yet been isolated.

The most interesting results are obtained when the zwitterion **XXIV** is employed. If water solutions of $\{[(\eta^5\text{-}C_5H_4COOH)(\eta^5\text{-}C_5H_4COO)Co]\ [(\eta^5\text{-}C_5H_4COOH)_2Co]\}[PF_6]$ are treated with alkali metal or ammonium hydroxides MOH ($M = K^+, Rb^+, Cs^+, [NH_4]^+$) in 1:1 stoichiometric ratio, the acid cation **XXIII** is partially deprotonated and the zwitterion **XXIV** is formed. The resulting solution contains, beside the zwitterion **XXIV**, the alkali or ammonium cation and the $[PF_6]^-$ anion. Upon crystallization **XXIV** forms nearly isomorphous supramolecular aggregates with the inorganic salts MPF_6 ($M = K^+, Rb^+, Cs^+, NH_4^+$) [35]. Alternatively, the same compounds can be prepared by treating water solutions of **XXIV** with the stoichiometric amount of the appropriate $[PF_6]^-$ salts, i.e. MPF_6 ($M = K^+, Rb^+, Cs^+, NH_4^+$). **XXIV**$[NH_4PF_6]$ and **XXIV**$[KPF_6]$ have been obtained also by grinding **XXIV** with the stoichiometric amount of the inorganic salt [36].

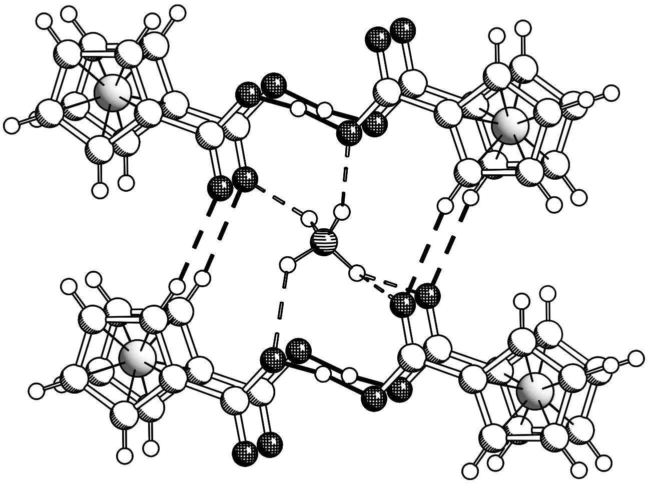

Fig. 16. The zwitterionic cages formed by **XXIV**: the N–H···O hydrogen bonds between the guest $[NH_4]^+$ cation and the surrounding O-atoms in the **XXIV**$[NH_4][PF_6]$ adduct.

The structural features of the four crystalline materials can be summarized as follows. The cations are encapsulated via either $M^+\cdots O$ interactions, in the cases of K^+, Rb^+, Cs^+, or N–H···O hydrogen bonds, in the case of the NH_4^+ cation, within a strongly nucleophilic cage formed by four molecules of **XXIV**. The walls of the cage are constituted of two *dimeric units* of **XXIV** held together by two O–H···O hydrogen bonds and by two C–H···O bonds, these latter involving the H-atoms of the C_5H_4-systems and the free lone pairs on the carboxylic oxygens. The K^+, Rb^+ and Cs^+ species are *quasi* isostructural and isomorphous with the ammonium salt aggregate (see Fig. 16).

The basic packing motif can be described as a sequence of C–H···O hydrogen bonded dimers encapsulating the cations, while the fluorine atoms belonging to the $[PF_6]^-$ anions form charge-assisted $C\text{–}H^{\delta+}\cdots F^{\delta-}$ interactions with the cyclopentadienyl ligands (see Fig. 17).

Single crystals of the anhydrous polymorphic modification of the neutral zwitterion $[(\eta^5\text{-}C_5H_4COOH)(\eta^5\text{-}C_5H_4\text{-}COO)Co^{III}]$ **XXIV** can also be prepared by *seeding* water solutions of **XXIV** with 'seeds' prepared by step-wise dehydration and subsequent phase transition of the hydrated species $[(\eta^5\text{-}C_5H_4COOH)(\eta^5\text{-}C_5H_4COO)Co^{III}]\cdot 3H_2O$ (see Fig. 18). A TGA experiment shows that the hydrated form reversibly releases one water molecule at 378 K, while the loss of the two remaining water molecules occurs at ca. 506 K and is immediately followed by a phase transition. Powder diffraction shows that the first dehydration leaves the crystal structure almost unchanged. Most remarkably, crystallization *from a water solution* of the powder obtained from TGA at 506 K in the presence of *seeds* (a small portion of *the same powder*) leads to the growth of single crystals of the anhydrous species. The structure of $[(\eta^5\text{-}C_5H_4COOH)(\eta^5\text{-}C_5H_4COO)Co^{III}]$ is based on a 1D

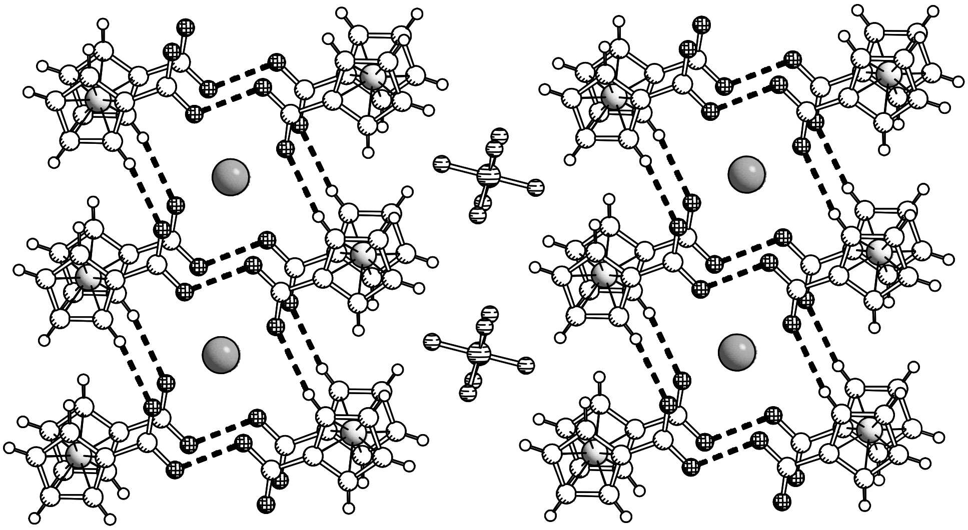

Fig. 17. Ball-and-stick representation of the cage arrangement in crystalline **XXIV**[M][PF_6]. The $[PF_6]^-$ anions pile up on both sides of the supramolecular cages and interact via C–H···F hydrogen bonds with the zwitterion molecules.

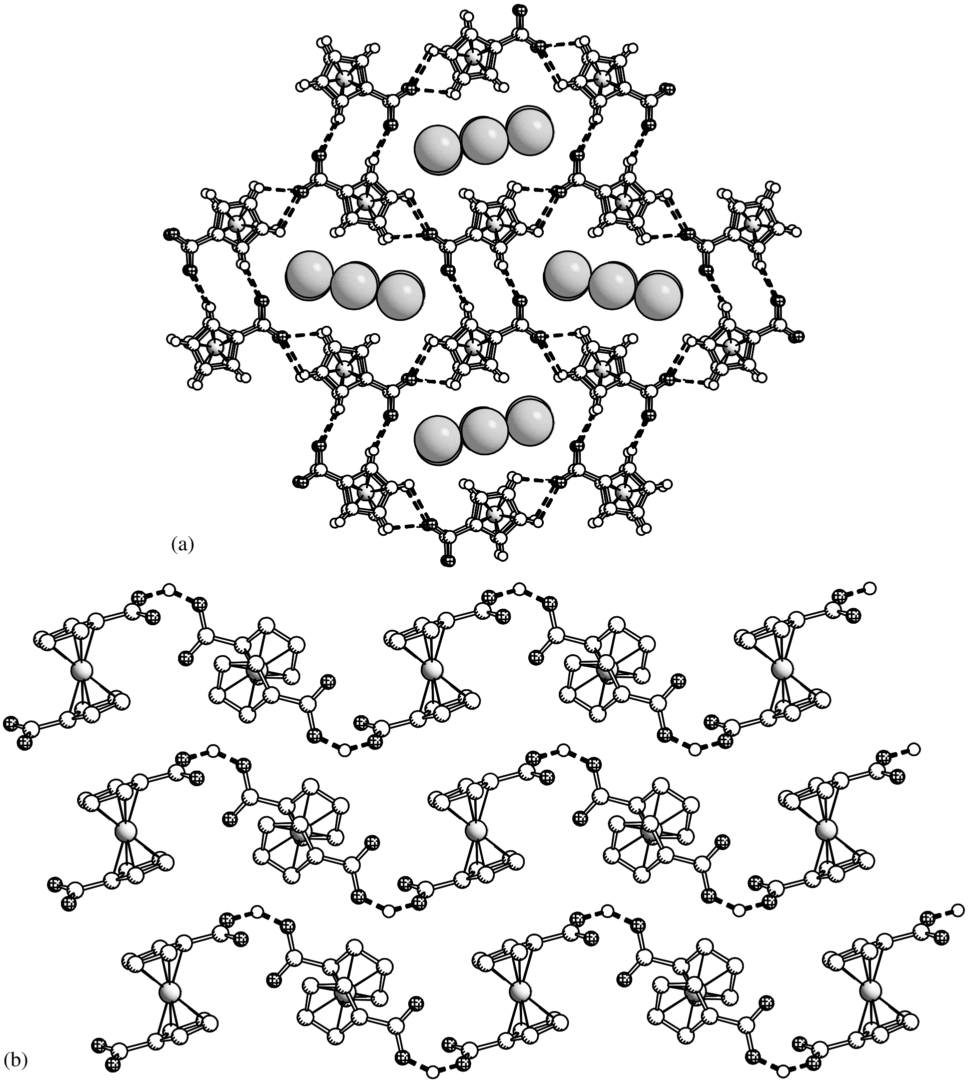

Fig. 18. (a) Comparison of the zwitterion arrangement in crystals of the hydrated species **XXIV**·$3H_2O$ and (b) the anhydrous **XXIV**, obtained by *seeding* the starting solution with 'seeds' prepared by step-wise dehydration and subsequent phase transition of the hydrated species.

network of O–H···O bonded zwitterion molecules (see Fig. 18). Comparison of the calculated and measured powder diffractograms of the anhydrous phase confirms that the powder obtained at 506 K and the single crystals precipitated at room temperature, after *seeding*, possess the same structure. It is useful to stress that, while crystallization, *in the presence of seeds of the anhydrous form*, leads to isolation of single crystals of the anhydrous material, *in the absence of seeds* the hydrated species is obtained [37].

The possibility of *switching* between neutral hydrogen bonded systems and charged systems is at the basis of the reversible gas-trap system obtained on reacting the cobalticinium zwitterion $[(\eta^5\text{-}C_5H_4COOH)(\eta^5\text{-}C_5H_4COO)\text{-}Co^{III}]$ with either acid and base vapors (HCl, CF_3COOH, HBF_4, and NH_3, NH_2Me, NMe_3) [38]. The salts resulting from the heterogeneous reactions contain the organometallic moiety either in its fully protonated form $[(\eta^5\text{-}C_5H_4COOH)_2Co^{III}]^+$ (in the reaction with acids) or in its fully deprotonated form $[(\eta^5\text{-}C_5H_4COO)_2Co^{III}]$– (in the reaction with bases). The two types of reactions imply the interconversion between neutral O–H O hydrogen bonding interactions and $^{(+)}$O–H X$^{(-)}$ and $^{(-)}$O H–N$^{(+)}$ interactions, respectively [38].

5. Conclusions and outlook

Molecular crystal engineering is supramolecular solid-state chemistry, and crystal engineers concentrate their efforts on developing synthetic strategies aimed to the preparation of periodic supermolecules. Engineering implies function-oriented design of the superstructure, selection of the building blocks (on the basis of their chemical and physical stability and of their extramolecular bonding capacity), their assembly and characterization to end with the evaluation of the properties of the resulting supramolecular aggregate. In order to be satisfactory, a supramolecular/crystal engineering synthetic strategy ought to be reproducible, hence the utilization of interactions that are strong and, at the same time, highly directional, such as hydrogen bonding, are favored for the assembly of molecular components. These interactions are transferable from crystal to crystal, and retain the same assembly-directing capacity even on changing the nature of the forces holding the building blocks together in the crystal. For these reasons the hydrogen bond is the interaction of choice in the engineering of both molecular and ionic crystals constructed from neutral molecules or molecular ions.

Since short intermolecular distances are often a *consequence* of other truly relevant interactions, such as those between ions in crystalline salts, it is useful to keep in mind that, even if the *energetic* contribution of the hydrogen bonding interaction is generally smaller than that arising from the Coulombic interaction between ions, the directionality is fully operative and can be thoroughly exploited to direct the recognition and assembly processes. Another useful notion is that the observation of a short hydrogen bond, i.e. of a short separation between donor and acceptor units, is not per se indicative of the existence of a stable aggregate of atoms: cations may be *required* to provide an external aid to keep ions of like charges together.

Furthermore, the simultaneous presence, in some of the cases discussed above, of fully deprotonated anions derived from a carboxylic acid, viz. of supposedly strong bases together *with* fully protonated acid molecules, may appear in contradiction with the ‘common-sense’ behavior of acids and bases. However, one should keep in mind that the acid-strength concept is relative to the strength of the proton acceptor, usually the solvent. In the solid state this concept cannot be applied lightly, because the interactions at work are of different nature than in solution.

With these *caveat* in mind, however, the utilization of organometallic building blocks in combination with the utilization of the prototypical supramolecular linker, that is to say the hydrogen bridge, constitute one of the most accessible tools to make crystalline materials and to attain complex properties or complex applications. It is not difficult to predict that the field of crystal engineering will see in the near future an increasing number of applications of organometallic building blocks in the construction of new solids.

Acknowledgements

We acknowledge financial support by the Universities of Bologna and Sassari, by MIUR and by bilateral exchange projects with Professor C. Elschenbroich (Marbug, Germany, Vigoni Program, DAAR-CRUI) and with Professor M. W. Hosseini (Strasbourg, France, Galileo Exchange).

References

[1] (a) See, for a general entry: D. Braga, F. Grepioni, A.G. Orpen (Eds.), Crystal Engineering: From Molecules and Crystals to Materials, Kluwer Academic Publishers, Dordrecht, 1999. (b) G.R. Desiraju (Ed.), Crystal Engineering: The Design of Organic Solids, Elsevier, Amsterdam, 1989. G.R. Desiraju Nature 412 (2001) 397.
[2] (a) J.M. Lehn (Ed.), Supramolecular Chemistry: Concepts and Perspectives, VCH, Weinheim, 1995;
(b) J.W. Steed, J.L. Atwood (Eds.), Supramolecular Chemistry, Wiley, Chichester, UK, 2000.
[3] (a) D.W. Bruce, D. O’Hare (Eds.), Inorganic Materials, Wiley, Chichester, UK, 1992;
(b) M.D. Hollingsworth, Science 295 (2002) 2410;
(c) D. Braga, J. Chem. Soc. Dalton Trans. 295 (2000) 3705.
[4] D. Braga, F. Grepioni, Acc. Chem. Res. 33 (2000) 601.
[5] G.R. Desiraju (Ed.), The Crystal as a Supramolecular Entity. Perspectives in Supramolecular Chemistry, Vol. 2, Wiley, Chichester, UK, 1996.
[6] D. Braga, G.R. Desiraju, J. Miller, A.G. Orpen, S. Price, Cryst. Eng. Commun. 4 (2002) 500.
[7] D. Braga, F. Grepioni, Coord. Chem. Rev. 183 (1999) 19.
[8] (a) D. Braga, F. Grepioni, P. Sabatino, G.R. Desiraju, Organometallics 13 (1994) 3532;

(b) D. Braga, F. Grepioni, G.R. Desiraju, Organometallics 17 (1998) 2669;
(c) D. Braga, F. Grepioni, G.R. Desiraju, J. Organomet. Chem. 548 (1997) 33.

[9] (a) G.R. Desiraju, T. Steiner (Eds.), The Weak Hydrogen Bond in Structural Chemistry and Biology, Oxford University Press, Oxford, 1999;
(b) D. Braga, F. Grepioni, K. Biradha, V.R. Pedireddi, G.R. Desiraju, J. Am. Chem. Soc. 117 (1995) 3156;
(c) M.J. Calhorda, Chem. Commun. 117 (2000) 801.

[10] (a) M.W. Hosseini, A. De Cian, Chem. Commun. 117 (1998) 727;
(b) C.B. Aakeroy, K.R. Seddon, Chem. Soc. Rev. 117 (1993) 397;
(c) L.J. Prins, D.N. Reinhoudt, P. Timmerman, Angew. Chem. Int. Ed. Engl. 40 (2001) 2382;
(d) A.M. Beatty, Cryst. Eng. Commun. 40 (2001) 51;
(e) G. Gilli, F. Bellucci, V. Ferretti, V. Bertolasi, J. Am. Chem. Soc. 111 (1989) 1023;
(f) G. Gilli, P. Gilli, J. Mol. Struct. 552 (2000) 1;
(g) T. Steiner, Angew. Chem. Int. Ed. 41 (2002) 48;
(h) G.R. Desiraju, Acc. Chem. Res. 35 (2002) 565.

[11] D. Braga, F. Grepioni, J. Chem. Soc. Dalton Trans. 35 (1999) 1.

[12] See, for example: (a) G. Aullon, D. Bellamy, L. Brammer, E.A. Bruton, A.G. Orpen, Chem. Commun. (1998) 653. (b) O. Felix, M.W. Hosseini, A. De Cian, J. Fischer Chem. Commun. (2000) 281. (c) S. Hanessian, M. Simard, S. Roelens, J. Am. Chem. Soc. 117 (1995) 7630. (d) R.E. Melendez, C.V.K. Sharma, M.J. Zaworotko, C. Bauer, R.D. Rodgers, Angew. Chem. Int. Ed. Eng. 35 (1996) 2213. (e) D. Papoutsakis, J.P. Kirby, J.E. Jackson, D.G. Nocera, Chem. Eur. J. 5 (1999) 1474.

[13] (a) D. Braga, F. Grepioni, J.J. Novoa, Chem. Commun. 35 (1998) 1959;
(b) D. Braga, L. Maini, F. Grepioni, F. Mota, C. Rovira, J.J. Novoa, Chem. Eur. J. 6 (2000) 4536;
(c) T. Steiner, Chem. Commun. 6 (1999) 2299;
(d) M. Mascal, C.E. Marajo, A.J. Blake, Chem. Commun. 6 (2000) 1591;
(e) P. Macchi, B.B. Iversen, A. Sironi, B.C. Chokoumakas, F.K. Larsen, Angew. Chem. Int. Ed. 39 (2000) 2719.

[14] D. Braga, F. Grepioni, G.R. Desiraju, Chem. Rev. 98 (1998) 1375.

[15] (a) G.A. Jeffrey, W. Saenger (Eds.), Hydrogen Bonding in Biological Structures, Springer, Berlin, 1991;
(b) M. Meot-Ner (Mautner), L.W. Sieck, J. Am. Chem. Soc. 108 (1986) 7525;
(c) M. Meot-Ner (Mautner), J. Am. Chem. Soc. 106 (1984) 1257.

[16] (a) D. Braga, F. Grepioni, New J. Chem. 106 (1998) 1159;
(b) D. Braga, F. Grepioni, J. Chem. Soc. Chem. Commun. 106 (1996) 571;
(c) D. Braga, F. Grepioni, in: J.M. Brown, P. Hofmann (Eds.), Topics in Organometallic Chemistry, Vol. 4, Springer, Berlin, 1999, p. 48.

[17] D. Braga, F. Grepioni, Structure and Bonding, in press.

[18] M.C. Etter, Acc. Chem. Res. 23 (1990) 120.

[19] (a) S.R. Marder, Inorg. Mater. 23 (1992) 115;
(b) N.J. Long, Angew. Chem. Int. Ed. Engl. 34 (1995) 21;
(c) T.J. Marks, M.A. Ratner, Angew. Chem. Int. Ed. Engl. 34 (1995) 155;
(d) D.R. Kanis, M.A. Ratner, T.J. Marks, Chem. Rev. 94 (1994) 195.

[20] (a) M.E. Davis, Chem. Eur. J. 3 (1997) 1745;
(b) C. Janiak, Angew. Chem. Int. Ed. Engl. 36 (1997) 1431;
(c) D.M.L. Goodgame, D.A. Grachvogel, D.J. Williams, Angew. Chem. Int. Ed. Engl. 38 (1999) 153;
(d) M. Eddaoudi, H. Li, O.M. Yaghi, J. Am. Chem. Soc. 122 (2000) 1391.

[21] (a) O. Khan (Ed.), Molecular Magnetism, VCH, New York, 1993;
(b) D. Gatteschi, Adv. Mater. 6 (1994) 635.

[22] (a) D. Braga, C. Bazzi, F. Grepioni, J.J. Novoa, New J. Chem. 23 (1999) 577;
(b) D. Braga, F. Grepioni, E. Tagliavini, J.J. Novoa, F. Mota, New. J. Chem. 23 (1998) 755;
(c) J.J. Novoa, I. Nobeli, F. Grepioni, D. Braga, New J. Chem. 24 (2000) 5;
(d)D. Braga, L. Maini, F. Grepioni, F. Mota, C. Rovira, J.J. Novoa, 6 (2000) 4536;
(e) D. Braga, E. D'Oria, F. Grepioni, F. Mota, J.J. Novoa, C. Rovira, Chem. Eur. J. 8 (2002) 1173.

[23] (a) D. Braga, A. Angeloni, F. Grepioni, E. Tagliavini, Chem. Commun. 8 (1997) 1447;
(b) D. Braga, A. Angeloni, F. Grepioni, E. Tagliavini, Organometallics 16 (1997) 5478.

[24] D. Braga, M. Eckert, M. Fraccastoro, L. Maini, F. Grepioni, A. Caneschi, R. Sessoli, New J. Chem. 26 (2002) 1280.

[25] D. Braga, L. Maini, L. Prodi, A. Caneschi, R. Sessoli, F. Grepioni, Chem. Eur. J. 6 (2000) 1310.

[26] D. Braga, A. Angeloni, L. Maini, A.W. Götz, F. Grepioni, New J. Chem. 6 (1999) 17.

[27] D. Braga, A. Angeloni, E. Tagliavini, F. Grepioni, J. Chem. Soc. Dalton Trans. 6 (1998) 1961.

[28] F. Grepioni, S. Gladiali, L. Scaccianoce, P. Ribeiro, D. Braga, New. J. Chem. 25 (2001) 690.

[29] (a) J.S. Miller, A.J. Epstein, Chem. Eng. News 73 (1995) 30;
(b) J.S. Miller, A.J. Epstein, W.M. Reiff, Chem. Rev. 88 (1988) 201;
(c) E. Coronado, J.-R. Galán-Mascarós, C.-J. Gómez-García, J. Ensling, P. Gütlich, Chem. Eur. J. 6 (2000) 552;
(d) E. Coronado, J.-R. Galán-Mascarós, C.-J. Gómez-García, V. Laukin, Nature 408 (2000) 447;
(e) J.S. Miller, A.J. Epstein, Chem. Commun. 408 (1998) 1319;
(f) M.B. Zaman, M.T. Tomura, Y. Yamashita, M. Sayaduzzaman, A.M.S. Chowdhury, Cryst. Eng. Commun. 408 (1999) 9.

[30] F. Takusagawa, T.F. Koetzle, Acta Crystallogr. B35 (1979) 2888.

[31] (a) J. Dunitz, J. Bernstein, Acc. Chem. Res. 28 (1995) 193;
(b) J. Dunitz, Acta Crystallogr. Sect. B B51 (1995) 619;
(c) N. Bladgen, R.J. Davey, Chem. Brit. 35 (1999) 44;
(d) D. Braga, F. Grepioni, Chem. Soc. Rev. 29 (2000) 229.

[32] D. Braga, L. Maini, F. Grepioni, A. De Cian, O. Félix, J. Fischer, M.W. Hosseini, New J. Chem. 7 (2000) 547.

[33] (a) D. Braga, L. Maini, F. Grepioni, Angew. Chem. 37 (1998) 2240;
(b) D. Braga, L. Maini, F. Grepioni, J. Organomet. Chem. 594 (2000) 101.

[34] D. Braga, L. Maini, F. Grepioni, C. Elschenbroich, F. Paganelli, O. Schiemann, Organometallics 20 (2001) 1875.

[35] D. Braga, L. Maini, M. Polito, M. Rossini, F. Grepioni, Chem. Eur. J. 6 (2000) 4227.

[36] D. Braga, L. Maini, M. Polito, F. Grepioni, Chem. Commun. 6 (2002) 2302.

[37] D. Braga, G. Cojazzi, D. Emiliani, L. Maini, M. Polito, R. Gobetto, F. Grepioni, Cryst. Eng. Commun. 4 (2002) 277.

[38] (a) D. Braga, G. Cojazzi, D. Emiliani, L. Maini, F. Grepioni, Chem. Commun. 4 (2001) 2272;
(b) D. Braga, G. Cojazzi, D. Emiliani, L. Maini, F. Grepioni, Organometallics 21 (2002) 1315.